MOLECULAR DYNAMICS SIMULATION OF ELECTROOSMOTIC & PRESSURE DRIVEN FLOWS IN NANOCHANNELS

By

MIAO MIAO

A thesis submitted in partial fulfillment of
the requirements for the degree of

MASTER OF SCIENCE

WASHINGTON STATE UNIVERSITY
School of Mechanical and Materials Engineering

August 2007

To the Faculty of Washington State University:

The members of the Committee appointed to examine the thesis of MIAO MIAO find it satisfactory and recommend that it be accepted.

_____
Chair

_____

_____

ACKNOLEDGEMENT

I would like to thank my advisor Dr. Prashanta Dutta for the research guidance, patience and understanding during the past four years. He has been making a difference of my life ever since the day I took his undergraduate heat transfer class. I am especially grateful for his great emotional and technical support during my internship period at Technip USA. To write a thesis while being a full time engineer is nothing like doing research while being the teaching assistant at school. Without him, this thesis is not possible. I would also like to thank Washington State University for providing me the financial support. Thirdly, many thanks go to my fellow lab mates for their mental support. In the end, I want to give the greatest appreciation to my parents.

MOLECULAR DYNAMICS SIMULATION OF ELECTROOSMOTIC & PRESSURE DRIVEN FLOWS IN NANOCHANNELS

Abstract

By Miao Miao, MS
Washington State University
August 2007

Chair: Prashanta Dutta

In order to deepen our understanding of pressure driven flow and electroosmotic flow in nano channels, a molecular dynamics simulation program was developed. Pressure driven flow happens due to a pressure gradient in the channel, whereas ions' movement due to an external electric field induces electroosmotic flow. For pressure driven flow, Lennard-Jones potential is simply used to simulate the van der Waals interaction. In addition to that, 3D Ewald Summation was employed to simulate the electrostatic interaction in electroosmotic flow.

Our system consists of 168 spherical rigid wall molecules and 2048 spherical liquid molecules. Channel length, width and height (L_x, L_y, L_z) are 4.588 nm, 4.588nm and 3.614nm respectively. Water molecules are sandwiched between top and bottom walls with a FCC structure as the initial configuration. In electroosmotic flow, there are 32 ions out of 2048 liquid molecules and 32 wall molecules are assigned charges in order to reach an electrostatic neutral condition.

A periodical boundary was added to simulate bulk flow in x and z direction. A Berendsen thermostat is also used to control the system temperature. Verlet neighbor hood list helps to reduce the computation time when calculating the pair interaction of molecules.

Six studies were conducted in this reearch: A comparison test of pressure driven flow with existing continuum theories; a parametric study of effect of external force in pressure driven flow; a limiting case study where the continuum theory completely breaks down in nano channels; a comparison study between simulation and continuum results of electroosmotic flow; a parametric study of electroosmotic flow with respect to effects of external electric field. Lastly we investigated the influence of density on electroosmotic flow.

From the results we do see small jumps of velocities near the channel wall. Flow velocity magnitude is proportional to the external field. We found that in a channel height of 5.5σ, parabolic velocity profile is no longer seen. It was also discovered that Poisson-Boltzmann theory fails to describe the ion distribution. In conclusion, our simulation results do agree with the existing molecular dynamics results from other research groups.

TABLE OF CONTENTS

LIST OF TABLES

LIST OF FIGURES

Dedication

This thesis is dedicated to the almighty God,
the creator of heaven and earth.

.

Nomenclature

$\vec{a}$	acceleration
D	dielectric constant of fluid
DM	dipole moment of the unit box
E	electric potential
E_x	external electric field
$\vec{F}$	force
$\vec{F}_{ij}$	Lennard-Jones pair force
h	height of the channel
i	molecule index
k	reciprocal lattice Vector
k_b	Boltzmann constant $\left(k_b = 1.38 \cdot 10^{-23} \frac{J}{K}\right)$
KE	kinetic energy
L_α	length of a unit box $(\alpha = x, y, z)$
m	mass of the particle
M	mobility
n	number of unit boxes
n^*	number of density
N	number of atoms
Na	Avogadro constant, $\left(Na = 6.023 \cdot 10^{23}\, mol^{-1}\right)$
NC	number of atoms per row in the unit box
$\vec{p}$	momentum

P	pressure
PE	potential energy
q_i	pair potential
r_i	position of molecule I
r_{ij}	intermolecular distance
r_{cut}	cutoff distance
r_{list}	cutoff distance for Verlet list
t	time
T	temperature
T_{inst}	instantaneous temperature
T_{ini}	initial temperature
$u_x(y)$	streaming velocity
U	total energy
V	Lennard-Jones pair potential
$\vec{V}_i$	total particle velocity
Vol	volume of unit box

Greek Symbols

α Gaussian width parameter

β ionic energy parameter

κ $[\cosh(\beta\psi_c / 2\psi_0)]^{-1}$

η rectilinear coordinate measured from center of channel in flow between plates

γ strain-rate

$\delta(...)$ dirac delta function

$\delta_y()$ step function

δt time step

ε Lennard-Jones energy parameter

ρ fluid density

$\tilde{\rho}$ charge density

$\tilde{\rho}(k)$ Fourier transformed charge density

μ continuum viscosity

ν_α viscosity $(\alpha = x, y, z)$

σ Lennard-Jones minimum separation distance

τ number of time steps

τ^* non-dimensional time

τ_T thermostat time constant

φ Coulomb's potential

ψ electric potential of ions

ψ_0 potential at surface of capillary

χ thermostat multiplier

ω reciprocal of Debye length

CHAPTER ONE

INTRODUCTION

1.1 Background

Today Mechanical engineers are not working alone, rather they are devoted to the collaboration with chemists, biologists and material scientists on nontraditional mechanical engineering projects. This trend started to develop due to the fast growing popularity of micro and nano scale mechanical devices in military and bio-medical applications such as separation and identification of biological and chemical species. While many people are focusing on the research in micro-scale, nanotechnology also begins to excel drastically.

Nanotechnology focuses on the design, synthesis, characterization and application of materials and devices on the nanoscale. Thanks to the development of nanotechnology, computer chips and other electronic devices have been scaled down million of times; more bio-chemical related researches were made possible; our homeland security is much stronger than ever.

Indeed many of the nano-scale research results have been applied successfully into production and manufacturing. Yet, plenty of technical difficulties remained to be undiscovered and puzzeled to the scientists and researchers. One of the biggest constraints in the nano field is the system efficiency problem; the other is the aid of visualizing in nano-scale or even smaller. Computer simulation in nano-scale was developed in accordance with these specific needs at this stage. The two main streams for computer simulation of fluid in nano-scales are Monte Carlo simulation and Molecular Dynamics Simulation. In addition, there are hybrid techniques as well. One of the advantages of Molecular Dynamics over Monte Carlo is that it gives a route to dynamical properties of the system [1].

Molecular dynamics simulation is a technique for computing the equilibrium and transport properties of a classical many body system. This simulation numerically solves the

Newton's equations of motion of a system on an atomistic scale of to obtain information about its time-dependent properties. Molecular dynamics simulation nowadays plays a very important role in the nano research fields. It is helping to solve the problems like carbon nano tube heat transfer problems, protein and DNA related research, material science study, etc.

Molecular dynamics is also widely used in hydrodynamic fields. Pressure driven flow was first simulated using molecular dynamic simulation. Great amount of attention has been drawn to the validity of continuum theory in nano scale. Not long after that, electroosmotic flow caught people's attention due to its advantages of precise control, no moving mechanical parts involved, etc. Field-driven flow applications nowadays are widely used in MEMS, Nano-electrical-mechanical-system, as well as fuel cell research [2]. Researchers have shown great interest in electroosmotic flow due to its affects on capillary electrophoresis, where the flow tends to counteract the electric field used to drag the DNA molecule. Such an application can be applied to the separation and identification of biological and chemical species [3,4].

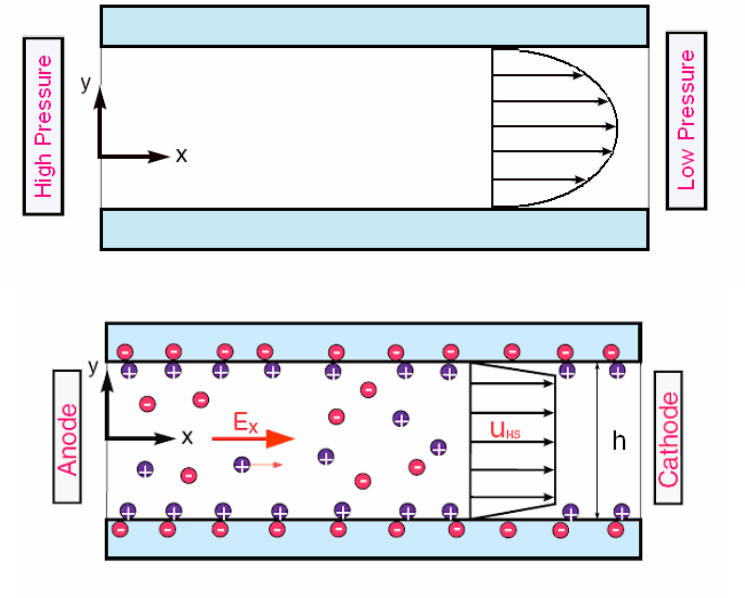

Figure 1 Schematics of pressure driven flow and electroosmotic flow in micro scale

(Picture courtesy: Horiuchi, K., Dutta, P., and Hossain, A.) [5]

Electroosmotic flow happens when electric potential are applied to an ionized fluid in channel with charged walls. The inner surface of the channel is negatively charged, the cations will be attracted to the surface, leaving more anions in the bulk region. When the electric field is applied, with the anode on one side and cathode on the other side, the anions are going to move to the anode. This movement will induce the water molecules' movement accordingly. One of the very exciting behaviors of fluid happening in micro channel is, unlike the velocity profile of pressure driven flow, we no longer see the parabolic profile in electroosmotic flow in micro scale. Rather, the velocity is more uniform like. Figure 1 shows the velocity profile of pressure driven flow and electroosmotic flow in micro channel.

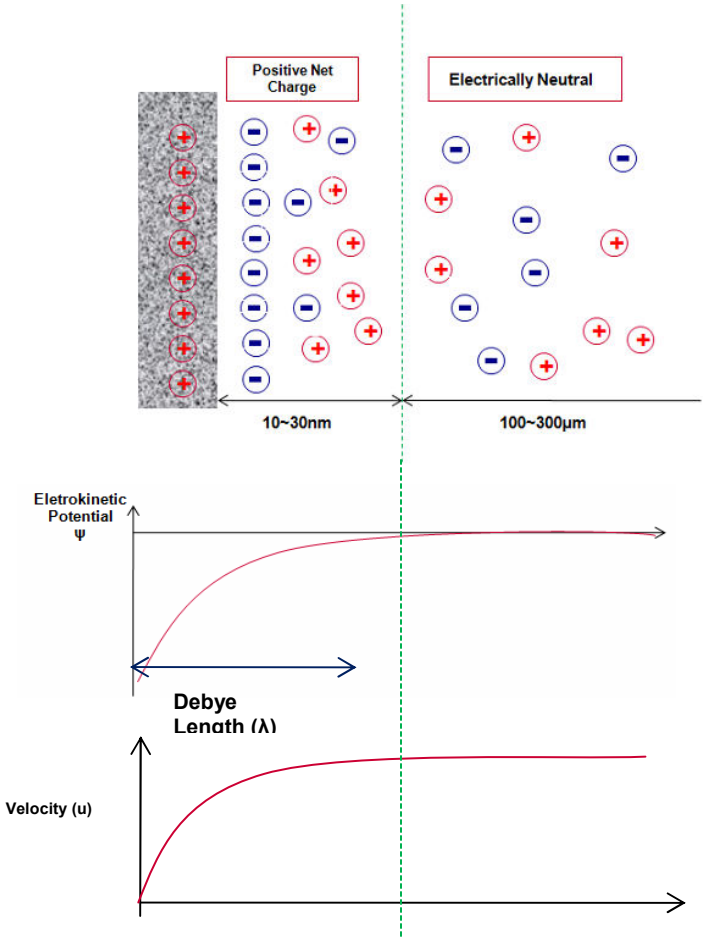

Figure 2 Schematics of electrokinetic potential and velocity profile along micro channel

In micro channels, as it shows in figure 2, the Debye length separates the two regions: the positive net charge region and the electronic neutral region. The Debye length is normally on the order of 10 nm to 30 nm. However, in a nano channel whose channel height is usually less than 10 nm, the Debye length will overlap. One of the main goals of this study is to investigate if the same electrokinetic potential distribution and "plug-like" velocity will reappear in the nano channels. Thanks to molecular dynamics, we are able to simulate the electroosmotic flow in nano channels.

1.2 Literature Survey

1.2.1 Molecular Dynamics Simulation

The first person that laid solid back group in studying the parameters for intermolecular interaction and potential is Lennard Jones. The potential is later named Lennard-Jones under his name [6]. Alder and Wainwrit developed the first simulation for a system of hard spheres around 1958 [7]. In this simulation, particles move at the same speed and undergo perfectly elastic collision. Several years later Rahman solved the equations of motion for a set of molecules by using the realistic Lennard-Jones potential of liquid argon [1]. The properties of Lennard-Jones models have been investigated in details by Velet, Nicolas, Gubbins, Streett, and Tildesley ever since then [1,8]. In 1971, Rahaman and Stillnger made the first attempt to model a diatomic molecular liquid using MD and this was the first MD program simulation ever developed [1]. With the rapid advance of computing capability, computer simulations of water molecules remain to be popular in recent years.

Classical Navier-Stokes hydrodynamics is known to describe macroscopic flows of simple fluids. In nano-scale where the state variables like temperature and density vary appreciably on a scale comparable to the molecular mean free path, these equations break down. Koplik *et al.* concluded that their system behaved in almost all respect like a continuum fluid in motion except the non-slip condition broke down near the contact line of a two-fluid system for an immiscible flow [9,10]. In 1995, Todd and Evans's simulation of a simple fluid undergoing Poiseuille flow in narrow channel presented significant instability in the density and stress profiles, although heat flux and velocity profiles were classical [11,12]. Later on, Travis *et al*. thoroughly examined the limitation of the Navier-Stokes hydrodynamic solution and it was

observed that in a channel of only 5.1 molecular diameters high, velocity profile depart significantly from the hydrodynamic prediction [13]. It was also found that velocity profile is independent of the externally applied pressure gradient and velocity no longer remained parabolic. In Travis and Gubbins's 2000 work, strong evidence was found that Newton's Law breaks down for very narrow pores and shear viscosity shows signs of singularities [13,14,15]. Once again, they discovered the slip boundary conditions. Jabbarazdeh and Tanner discovered that the degree of slip is dependent of the shear rate [1]. Another flow that drew great attention is the Couette flow. Unlike pressure driven flow, there is no explicit external field appearing in the equations of motion. Hu *et al*. in 1996 simulated the Couette flow, which was induced by translating one, or both channel walls along the flow direction [16].

Temperature of the system plays a very important role in the simulation. Berendsen *et al*. [17,18] in 1987 proposed the method of controlling the kinetic energy to achieve constant temperature, which implies rescaling molecular velocities at regular intervals Nose has developed another thermostat [19, 20], by introducing an additional degree of freedom and employing appropriate equations of motion. He showed that one may generate configurations belonging to either canonical or the constant temperature-constant pressure ensemble [21,22]. In 1980 Andersen proposed the constant temperature method [23]. The system is coupled to a heat bath that imposes the desired temperature. He allowed volume to fluctuate, determining its average by the balance between the internal pressure and the externally set pressure.

1.2.2 Electroosmotic Flow

Electroosmotic flow (often abbreviated EOF) is defined as the motion of water through very narrow channels caused by an electrical voltage applied across the channel. Electroosmotic flow happens when electric potential are applied to an ionized fluid in channel with charged walls. The inner surface of the channel is negatively charged, the ions will be attracted to the surface, leaving more anions in the bulk region. When the electric field is applied, with the anode on one side and cathode on the other side, the anions are going to move to the anode. This movement will induce the water molecules' movement accordingly.

Reuss first reported the exsitance of electroosmotic flow in Proceedings of the Imperial Society of Naturalists of Moscow in 1809. He demostrated the phenomena that water flow could be generated in a plug of clay by applying an electric voltage.

Helmholtz in 1879 developed the double layer theory, which related analytically the electrical and flow parameters of Newton kinetic transport. Smoluchowski, in 1902, expanded on Helmoholtz's double layer theory velocity in the capillary theory. In 1964, Burgreen and Nakache first published their analytical study for Newtonian kinetic flow in very fine capillary channels of rectangular cross section [24]. Electroosmotic flow is widely applied in the scientific field due to its efficiency and accuracy of inducing micro flow in micro fluidic devices.

Micro scale Electroosmotic flow was studied and characterized by numerical, analytical and experimental method. However, nano-scale electroosmotic flow remains to be unknown to the world until molecular dynamics simulation was used to simulate flows happening at ultra small channel height, usually on the order of several molecular radii.

In 2002, Freund proposed the Electroosmotic flow model by molecular dynamics [25]. Water molecules were modeled by SPE/C potential and Cl^- was modeled as point charges. They

found general agreement of ion distribution with Poisson-Boltzmann theory except that ions seems to be more attracted to the wall. The ion concentration was found 80 to 100 percent higher in distributed elementary charge case and uniformly charged wall case respectively. They also pointed out that velocity distribution is almost parabolic in the mid plane of the channel, but it showed a flattened pattern near walls. Non-Slip boundary condition was not seen in their simulation. For their uniformly distributed partial charges case, they found zero mean velocity in the first layer of the channel.

Qiao and Aluru simulated electroosmotic flow in nano channels whose channel width varies from 0.95 to 10.00 nm by both molecular dynamics method and continuum simulations [26]. They presented the same mismatching ion distribution near wall. It was found that continuum flow theory could be applied to predict the bulk flow behavior in a channel as small as 2.22 nm. Nevertheless, the continuum theory breaks down in the entire channel for electroosmotic flow in a 0.95 nm channel. They concluded that this difference was due to that continuum theory neglected the effects by finite size of ions and discreteness of the solvent molecules.

Kim and Darve in 2006 deepened the study of molecular dynamics simulation to study electroosmotic flows inside charged nano channels with varying surface roughness on the order of Debye length [27]. The very fundamental difference between fluid flow in nano channels and in micro channel is the strong liquid-wall interaction in nano scale. This is due to the increase of surface-to-volume ration caused by the dramatic decrease of channel size. So special attention needs to be drawn to the properties of the wall such as the surface roughness in nanotechnology research.

The channel walls were modeled shaping like the step function type with amplitude, period and symmetry changing. Again the walls were negatively charged and only positive ions

were presented in the channel for simplicity. They discovered that similar shape density distribution as the smooth wall cases except where at the “wall steps”. The ionic distribution is not consistent with the Boltzmann distribution. The zeta potential decreases with an increasing amplitude and a decreasing period of surface roughness and so as the flow rate. Qiao in March 2007 also presented his research interests in the surface roughness of channel wall. His results indicate that the electroosmotic flow will be affected once the thickness of the electrical double layer is on the same order of the height of surface roughness [28].

1.3 Motivation for This Work

The biggest puzzle in nano-scale fluid mechanics study is about the validity of hydrodynamics theory. Traditional continuum theory such as Navier-Stokes equation is not applicable to the nano-scale problem due to the inappropriate assumptions. Navier-Stokes equation assumes that State variables like density and temperature do not vary significantly over intermolecular distance. However, state variables do vary appreciably on a scale comparable to the molecular mean free path and thus this is not an appropriate assumption in the nano scale. People had tried to observe flows happening in nano channels, however due to the limitation of the visualization instrument, we are still incapable to visualize nano-scale phenomenon.

A numerical method was developed to help predict the fluid behavior in nano size channel, which is called the Molecular Dynamics Simulation. Molecular dynamics uses Newton's equation of motion to predict the trajectory of each molecule in a system. It can provide detailed information on fluid molecules' interaction and thus present the simulated behavior of fluid in nano channels.

The objective of this study is to simulate and characterize pressure driven flow and electroosmotic flow by molecular dynamics simulation. In Chapter 2, the governing equations and methodology were given. In Chapter 3 and 4, some numerical approaches were discussed in details. Chapter 5 presents the results as well as parametric study of both the pressure driven flow and electroosmotic flow. The last chapter draws the important conclusions of the thesis.

CHAPTER TWO
METHODOLOGY

2.1 Molecular Dynamics Simulation

2.1.1 Governing Equations

The molecular dynamics simulation was developed based on the well know Newton's second law, in other words, equation of motion,

$$\vec{F}_i = m_i \vec{a}_i \tag{2.1}$$

where $\vec{F}_i$ is the force exerted on molecule, m_i stands for the molecule mass and a_i is the acceleration. Force can also be defined as the gradient of potential energy, which can be written as

$$\vec{F}_i = -\nabla_i V \tag{2.2}$$

By combining these two equations we can relate the potential energy with the motion of the molecules,

$$-\frac{dV}{d\vec{r}_i} = m_i \frac{d^2\vec{r}_i}{dt^2} \tag{2.3}$$

where V is the potential energy of the system. This relationship is the fundamental understanding of molecular dynamics simulation.

By applying Newton's Law of motion again, can we integrate the motion for all the particles in our system.

$$\vec{V} = \vec{V}_o + \frac{d^2\vec{r}_i}{dt^2}\delta t \tag{2.4}$$

$$\vec{r}_i = \vec{r}_0 + \vec{V}\delta t \tag{2.5}$$

It can be understood that in order to calculate the trajectory of a particle, all the information needed is the initial position and initial velocities, which are the initial configuration of the system. We would also need the acceleration of each particle, which is determined by the potential energy function.

When consider the simple case of one atomic system, which has N atoms. The potential energy can be written as a summation of terms depending on the coordinates of individual atoms, pairs, triplet etc [1]

$$V = \sum_i V_1(\vec{r}_i) + \sum_i \sum_{j>i} V_2(\vec{r}_{i,}\vec{r}_j) + \sum_i \sum_{j>i} \sum_{k>j>i} V_3(\vec{r}_i, \vec{r}_j, \vec{r}_k) + \ldots \tag{2.6}$$

where $V_1(r_i)$ is the effect of an external field on the system, the second term is a summation over all distinct pairs i and j and third term is a summation over particle i, j and k and so on. It was found that any summation over triplets of molecules could be very computational expensive and pairwise approximation actually is able to give a good description of the liquid properties. So equation (2.6) can be rewritten as

$$V = \sum_i V_1(\vec{r}_i) + \sum_i \sum_{j>i} V_2(\vec{r}_{i,}\vec{r}_j) \tag{2.7}$$

This is another major methodology in order to perform an effective molecular dynamic simulation, that is we only consider the molecular interaction pairwise.

2.1.2 Integration Algorithms

The motion of integration is done numerically by special finite difference methods. Variety of different methods are available, however, accuracy and efficiency vary from case to case. The major algorithms being used are: Verlet algorithm, Leap-frog algorithm, Gear predictor-corrector algorithm, etc.

Verlet Algorithm, that was first developed by Verlet in 1967 [8] is the most widely used method and in fact it is a finite difference method. The algorithm is briefly introduced as following:

The equation for advancing the position is

$$\vec{r}(t+\delta t) = 2\vec{r}(t) - \vec{r}(t-\delta t) + \delta t^2 \vec{a}(t) \tag{2.8}$$

After Taylor expansion, it can be written as

$$\vec{r}(t+\delta t) = \vec{r}(t) + \delta t\vec{V}(t) + (1/2)\delta t^2 \vec{a}(t) + \ldots \tag{2.9}$$

$$\vec{r}(t-\delta t) = \vec{r}(t) - \delta t\vec{V}(t) + (1/2)\delta t^2 \vec{a}(t) - \ldots \tag{2.10}$$

The velocity can be obtained by

$$\vec{V}(t) = \frac{\vec{r}(t+\delta t) - \vec{r}(t-\delta t)}{2\delta t} \tag{2.11}$$

The simplicity and its modest requirement of storages are the advantages of this program. However, the algorithm's precision is one of the main drawbacks.

Another commonly used algorithm is Leap-frog algorithm, which is a modified version of Verlet algorithm. This algorithm is used in this study based on its good computational efficiency and accuracy. A schematic of this algorithm is shown in figure 3 [1].

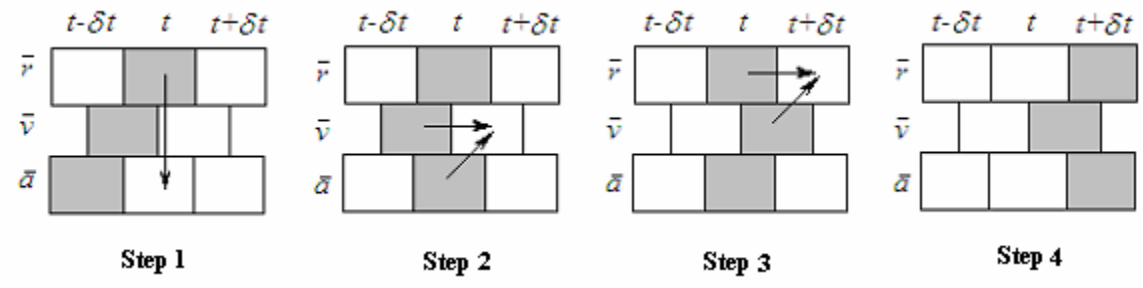

Figure 3 Schematic of half-step "Leap-frog" scheme

In the first step, acceleration at time t is calculated from taking the derivatives of the Lennard-Jones potential based on the location of all the molecules. Then together with velocity at $t-\frac{1}{2}\delta t$, the new velocity is calculated at time $t+\frac{1}{2}\delta t$,

$$\vec{V}(t+\frac{1}{2}\delta t)=\vec{V}(t-\frac{1}{2}\delta t)+\vec{a}(t)\delta t \tag{2.12}$$

The position of each molecule at time $t+\delta t$ is calculated based on the previous position and the velocity at $t+\frac{1}{2}\delta t$,

$$\vec{r}(t+\delta t)=\vec{r}(t)+\vec{V}(t+\frac{1}{2}\delta t)\delta t \tag{2.13}$$

having both $\vec{V}(t+\frac{1}{2}\delta t)$ and $\vec{V}(t-\frac{1}{2}\delta t)$, we calculate current step velocity as

$$\vec{V}(t)=\frac{1}{2}\left[\vec{V}(t-\frac{1}{2}\delta t)+\vec{V}(t+\frac{1}{2}\delta t)\right] \tag{2.14}$$

The same procedure will be repeated again at the next time step for all the liquid molecules and ions.

The disadvantage of this program is that velocities and positions are not calculated at the same time. So kinetic energy and potential energy can not be calculated at the same time either. Gear predictor-corrector algorithm was implemented in our program for a benchmarking run. It was found that Leap-frog algorithm was better in terms of calculation efficiency and precision.

2.2 Potentials

2.2.1 van der Waal Forces

From the chemistry point of view, particle interactions can be categorized into four different types, ionic interactions, hydrogen bonds, dipole-dipole interactions and van der wall interactions. In our simulation, we consider water molecules interaction to be van der Waal interactions solely. The Lennard-Jones potential is often used as an approximate model for the Van der Waals force as a function of distance, which describes the interaction between two uncharged molecules or atoms. It was first proposed by John Lennard-Jones at Bristol University in 1931 [1]. This potential has both repulsion and attraction parts and can be represented as

:

$$V = 4\varepsilon\left(\left(\frac{\sigma}{r_{ij}}\right)^{12} - \left(\frac{\sigma}{r_{ij}}\right)^{6}\right) \tag{2.15}$$

where ε and σ are Lennard-Jones interaction strength and Lennard-Jones minimum separation distance respectively, which are unique for each molecule, r_{ij} is the intermolecular distance. One way of finding these parameters is to use the quantum chemistry calculation; another way is from the experimental data. The first term represents the repulsion and the second term represents the attraction.

Following is a picture that illustrates Lennard-Jones potential with respect to intermolecular distance. The slope on the graph is the derivative of the potential, in other words, the Lennard-Jones force. The dashed line is the equilibrium point between two molecules where force is zero. On the left side of the equilibrium line, we see all negative slopes and since force is

the negative derivative of potential, the force on the left is actually positive forces, which is the repulsive force. Attractive forces are all on the right side of the equilibrium line and it vanishes quickly with respect to the intermolecular distance. Due to this phenomenon, we could intentionally set a cutoff distance r_{cutoff}, beyond which point, where we assume that Lennard-Jones potential is negligible. Thus we can intentionally set a cutoff sphere for each molecule. If $r_{ij}>r_{cutoff}$, the force between these pair is not considered in the calculation. A detailed explanation can be found in Chapter 3.

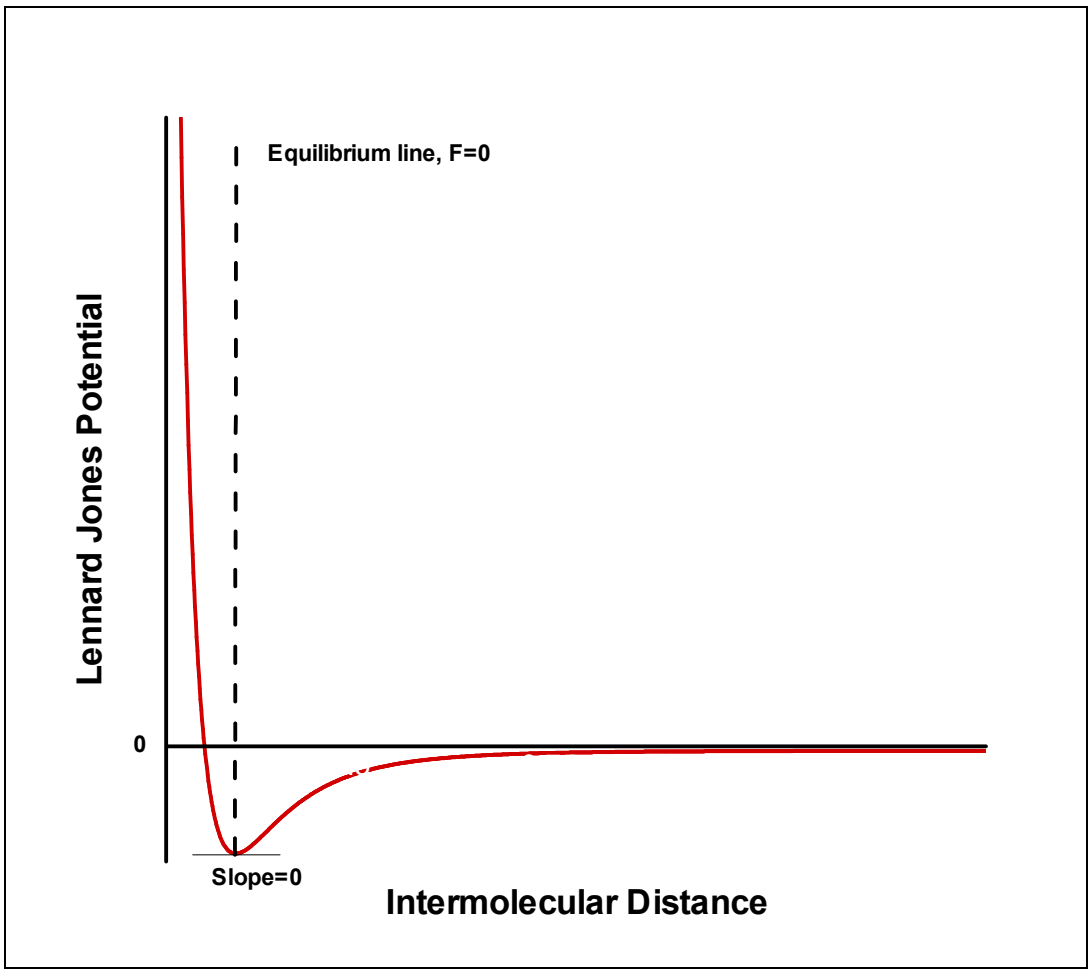

Figure 4 Lennard-Jones potential with respect to intermolecular distance

Force is defined as the negative derivative of potential, $\vec{F} = -\nabla V$. If we take the gradient of the above equation (2.15), we can get the Lennard-Jones force equation:

$$\vec{F}^{LJ}(r) = \frac{6}{r_{ij}}\left(2\frac{C_{12}}{r_{ij}^{12}} - \frac{C_6}{r_{ij}^{6}}\right) \tag{2.16}$$

where $C_{12} = 4\varepsilon\sigma^{12}$ and $C_6 = 4\varepsilon\sigma^{6}$.

The Lennard-Jones parameters are shown in Table 1. They are obtained from Gromacs force field [26].

Table 1 Lennard-Jones Parameter

L-J pair	C_6 (kJ nm^6/mol)	C_{12} (kJnm^{12}/mol)	σ (nm)
Water-water	0.2617E-2	0.2633E-5	0.317
Water-wall	0.6211E-2	0.7644E-5	0.327
Water-ion	0.6011E-2	0.1678E-4	0.375
Ion-ion	0.1380E-1	0.1069E-3	0.445
Ion-wall	0.1426E-1	0.4871E-4	0.388

Newton's third law states that for every action (force) in nature there is an equal and opposite reaction. Based on the law we can define molecular forces for both i and j particles.

$$\vec{F}_{ij} = \vec{F}_i = -\vec{F}_j \tag{2.17}$$

Due to reason that the system is consists of fluid molecules and solid molecules, the total force on one molecule can be represented as the summation of force obtained from pair interaction between fluid-fluid interaction, solid-fluid interaction and effects from the external field.

$$\vec{F}_{tot} = \sum \vec{F}_{f-f} + \sum \vec{F}_{s-f} + \vec{F}_e \tag{2.18}$$

2.2.2 Electrostatic Interaction

2.2.2.1 Introduction

Lennard-Jones potential is categorized as the short ranged potential, that is, the potential on atom *j* cause by atom *i* vanishes when their separation distance r_{ij} is larger than a cutoff distance r_{cutoff}. However, not all the molecular interactions are short ranged. For example, Electrostatic interaction's effects do not vanish within a cutoff distance. Figure 4 shows that Lennard-Jones model can be truncated at about 2.5 Lennard-Jones diameters, whereas the Coulomb potential at 5 Lennard-Jones diameters does not even come close to zero [29].

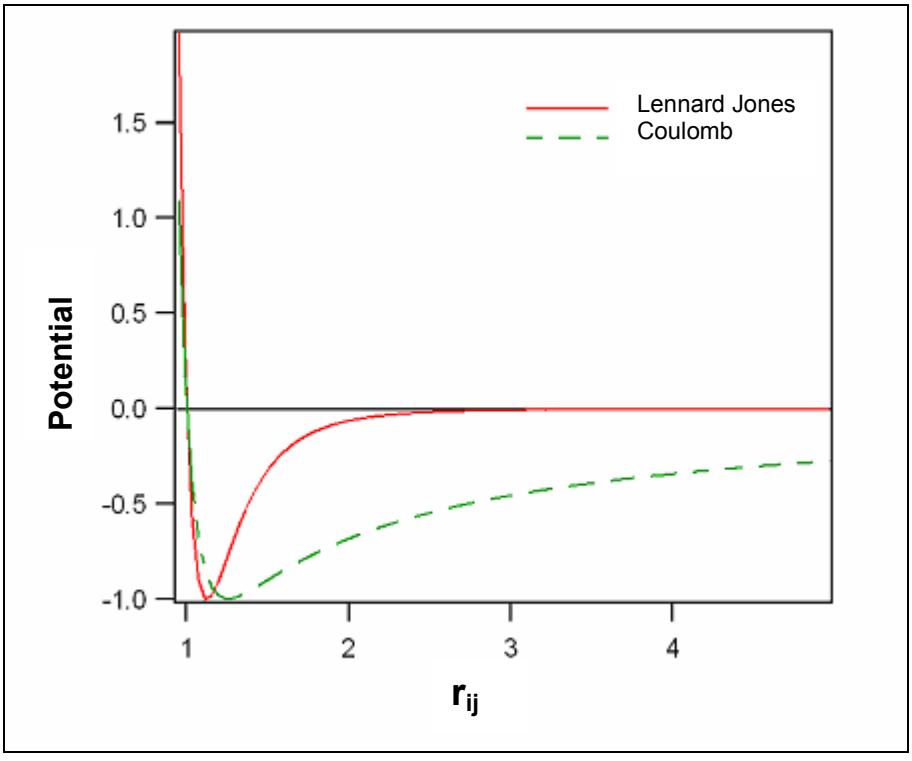

Figure 5 Comparison between Lennard-Jones potential and Coulomb potential

It can be simply understood that this is caused by the fact that electrostatic interaction presents in terms of 1/r. This can be recognized from the Coulomb's law (Eq. 2.19), but Lennard-Jones potential is in terms of $1/r^6$

Special treatment needs to be carried out to model the long-range forces. Two common approaches are taken to solve this problem. One is to divide the domain into lattice and do a lattice summation by using better techniques, which can help with the convergence. The other way is to simulate the media as dielectric continuum that responds to the fluctuation in the simulated system. The former method is called the Ewald sum. A detailed explanation of the mathematics can be found in this chapter.

Ewald Summation was first developed by researchers in the crystallographic community. Due to the periodicity in the lattice, Fourier series is applied. (Appendix 2 explains the discrete Fourier series.) It was then applied to calculate electrostatic potential due to their commonalties in reciprocal term, Fast Fourier Transforms and electron density distribution.

Now let us see how Fourier series was chosen first. Consider an electrostatic neutral system of N ions in a unit box of length L. After periodic boundary condition in x, y and z direction is applied, the Coulomb potential is given as:

$$E = \frac{1}{2} \sum_{i,j=1}^{N} \sum_{n \in Z^3}^{'} \frac{q_i q_j}{\left| r_{ij} + nL \right|} \tag{2.19}$$

where q_i and q_j are pair ions, r_{ij} is the distance between ions. This summation takes care of all particles' interaction and its periodic images in **n** unit boxes. Note prime here means that when **n**=0, all i=j terms must be omitted.

Ewald summation is conditionally convergent. Its convergence depends on the order how the summation is added up, its shape and nature of the surrounding medium. From equation (2.19) we know that electrostatic potential is a function of 1/r, which varies dramatically at small r and decays very slowly at big r, which makes the calculation impractical. People came up with the idea to represent 1/r with a different expression:

$$\frac{1}{r} = \frac{f(r)}{r} + \frac{1-f(r)}{r} \tag{2.20}$$

$f(r)$ should serve two functions, one is to have $\frac{f(r)}{r}$ negligible beyond the cutoff distance, another to make $\frac{1-f(r)}{r}$ vary slowly at all r.

It was found that the complementary error function ($erfc(r) = 2\pi^{-1/2}\int_r^\infty dt \exp(-t^2)$) is a good choice for $f(r)$. For atom pairs in the direct lattice, direct calculation was done, whereas Fast Fourier Transform was used to calculate the later one [29,30,31].

2.2.2.2 Literature Survey

There are several different modified Ewald summation methods, such as PME (particle mesh ewald) [32], P^3M (Particle-particle-particle-mesh) [33], SPME (smooth particle mesh ewald) [34]. Particle-mesh Ewald (PME) is a popular method to model electrostatic forces of a system with periodic boundary condition. There are many modified versions of PME models for higher efficiency and smoother results. Parry first introduced a two-dimensional Ewald summation (EW2D) and it was found to be the most accurate method. However Yeh pointed out that EW2D model is computational expensive [29, 36, 37]. So a EW3DC model was developed

accordingly, which basically is the regular EW3D method with a correction term [35]. The final potential energy contains a real space sum plus a reciprocal space sum minus a self-term plus the surface term[38, 39, 40, 41]. The regular EW3D equation is following:

$$U = (\frac{1}{2}\sum_{i=1}^{N}\sum_{j=1}^{N}\sum_{|n|=0}^{\infty}{}' q_i q_j \frac{erfc(\alpha|r_{ij}+n|}{|r_{ij}+n|}) + (\frac{1}{2\pi Vol.}\sum_{i=1}^{N}\sum_{j=1}^{N}\sum_{k\neq 0} q_i q_j (\frac{4\pi^2}{k^2})\exp(-\frac{k^2}{4\alpha^2})\times\cos(k\cdot r_{ij})) \\ -\left(\frac{\alpha}{\sqrt{\pi}}\sum_{i=1}^{N} q_i{}^2\right) + J(DM,P) \tag{2.21}$$

where J(DM,P) is a shape-dependent term, where DM is the total dipole moment of the unit cell, P stands for the geometry.

2.2.2.3 Mathematics Model

Yeh and Berkowitz [29] has shown that a correction term can be added to EW3D to obtain the correct limiting behavior in the limit of an infinitely thin slab, in other words, nano channel. Smith [35] in 1981 discovered that the EW3DC can be simplified as

$$U = (\frac{1}{2}\sum_{i=1}^{N}\sum_{j=1}^{N}\sum_{|n|=0}^{\infty}{}' q_i q_j \frac{erfc(\alpha|r_{ij}+n|}{|r_{ij}+n|}) + (\frac{1}{2\pi V}\sum_{i=1}^{N}\sum_{j=1}^{N}\sum_{k\neq 0} q_i q_j (\frac{4\pi^2}{k^2})\exp(-\frac{k^2}{4\alpha^2})\times\cos(k\cdot r_{ij})) - \\ \frac{2\pi}{3V}|q_i r_i|^2 - \left(\frac{\alpha}{\sqrt{\pi}}\sum_{i=1}^{N} q_i{}^2\right) \tag{2.22}$$

The force on particle i, is obtained by differentiating the potential energy U with respect to ri,

$$F_i = -\frac{\partial}{\partial r_i}U \tag{2.23}$$

The last term of equation (2.22) will disappear after the differentiation because it is not in terms of r_i. The forcing formula can be written as

$$F_i = F_i^{(r)} + F_i^{(k)} + F_i^{(c)} \tag{2.24}$$

where we call $F_i^{(r)}$ real space ewald term or R-Ewald, $F_i^{(k)}$ k space ewald term or K-Ewald and $F_i^{(c)}$ C space ewald, or C-Ewald

- R-Ewald

$$E^{(r)} = \frac{1}{2}\sum_{i=1}^{N}\sum_{j=1}^{N}\sum_{|n|=0}^{\infty} q_i q_j \frac{erfc(\alpha|r_{ij}+mL|)}{|r_{ij}+mL|} \tag{2.25}$$

$$\vec{F}_i^{(r)} = q_i \sum_j q_j \sum_{m\in Z^3} \left(\frac{2\alpha}{\sqrt{\pi}}\exp(-\alpha^2|r_{ij}+mL|^2) + \frac{erfc(\alpha|r_{ij}+mL|)}{|r_{ij}+mL|}\right)\frac{r_{ij}+mL}{|r_{ij}+mL|^2} \tag{2.26}$$

where r_{ij} - intermolecular distance between particle I and j.

q_i, q_j – ion and wall charges

L – unitbox length

α – Gaussian width parameter governs the convergence of real space and reciprocal space sums. α is usually chosen to be 5/L, where L is the unit box length which various between (40 to 100 Å). α in this case is 0.13 $Å^{-1}$. Also we only consider the molecules in the unit box here, $|m| = 0$.

- C-Ewald

Smith [35] showed that if a geometry of a rectangular plate or disk which are infinitely thin in y direction are used as a summation geometry in the Ewald summation, then the shape-dependent term J(DM,P) is given by

$$J(DM,P)=\frac{2\pi}{V}DM^2=\frac{2\pi}{V}(\sum_{i=1}^{N}q_i r_i)^2 \tag{2.27}$$

The contribution of force from this term is:

$$\vec{F}_{x,i}=\vec{F}_{z,i}=0 \tag{2.28}$$

$$\vec{F}_{y,i}=-\frac{\partial J(DM,P)}{\partial z_i}=-\frac{4\pi q_i}{V}DM_y=-\frac{4\pi q_i}{V}\sum_{i=1}^{N}q_i r_{y,i} \tag{2.29}$$

where DM_y is the y component of the total dipole moment of the simulation cell.

- K-Ewald

K-Ewald is also called the reciprocal term. The reciprocal space uses multidimensional piecewise interpolation for evaluating the Fourier terms, with grid size and number of terms chosen to achieve the desired accuracy.

$$E^{(K)}=\frac{1}{2L^3}\sum_{K\neq 0}\frac{4\pi}{k^2}\exp(-\frac{k^2}{4\alpha})\left|\widetilde{\rho}(k)\right|^2=\frac{1}{2\pi V}\sum_{i=1}^{N}\sum_{j=1}^{N}\sum_{K\neq 0}q_i q_j(\frac{4\pi^2}{k^2})\exp(-\frac{k^2}{4\alpha})\times\cos(\kappa r_{ij}) \tag{2.30}$$

$$\vec{F}^{(K)}=\frac{q_i}{L^3}\sum_j q_j\sum_{k\neq 0}\frac{4\pi\kappa}{k^2}\exp(-\frac{k^2}{4\alpha^2})\sin(\kappa r_{ij}) \tag{2.31}$$

where $\widetilde{\rho}(k)$ is Fourier transformed charge density

CHAPTER THREE
NUMERICAL TRICKS

3.1 Periodic Boundary

In order to simulate bulk flow and minimize the surface effects, normally periodical boundary condition is applied in the molecular dynamics simulation. First, a check is applied at the system boundary to examine if any molecule is exiting the boundary. If it is true, then the molecule is going to be shifted back to the other side of the system with the same velocity magnitude and direction.

The mathematical expression can be represented as:

$$\vec{r}_i = \vec{r}_i + L_i \tag{3.1}$$

where r_i is the location of the molecule outside of the boundary, L_i is the length of the system. The next figure illustrates how the visual periodical boundary is constructed.

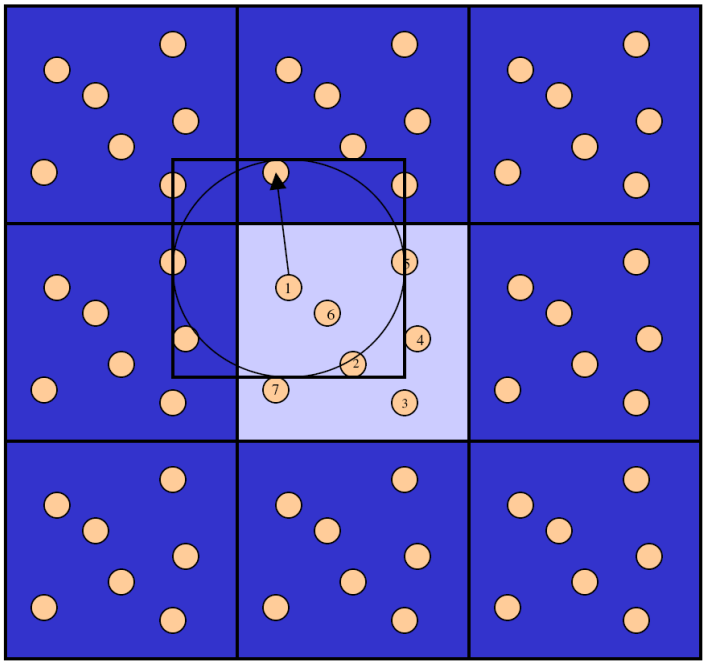

Figure 6 Schematic of periodic boundary condition

3.2 Thermostat

Thermostat is another useful tool in the molecular dynamics simulation, which regulates the temperature of the system. In a special case, when the wall molecules are assumed to be stationary for calculation simplicity, heat can not be carried out of the system. In order to keep temperature stable, thermostat is applied. In this simulation, the Berendsen thermostat [1]is applied .

$$\chi = \sqrt{1 + \frac{\Delta t}{\tau_T}\left(\frac{T_{ini}}{\mathrm{T}_{inst}} - 1\right)} \tag{3.2}$$

where the instantaneous kinetic temperature is defined as

$$T_{inst} = \frac{2KE}{3k_b} \tag{3.3}$$

τ_T is the length of the thermostat time step and it is used to adjust the effectiveness of the thermostat and it is found appropriate to be 0.4ps [1].

Δt is the length of the time step of the whole simulation.

Thermostat is only applied on the y and z direction because there is a finite streaming velocity in the x direction. In order to control the temperature on the x direction, we need to first find the average or streaming velocity profile. However, when the velocity is comparable to the thermal velocity, it is not necessary of tracking the peculiar velocity. To thermostat only the y and z directions should be sufficient in controlling the temperature. The heat transfer between the three degrees of freedom makes sure the total system temperature maintain the same [42]. Wei Zhu *et al*. had proved that the heat transfer rate is very rapid.

3.3 Neighbor List

To improve the calculation efficiency, a neighbor list is constructed for bookkeeping molecules' neighbor. This list checks for interactions with only those staying within an imaginary sphere of radius $r_{list} = 3\sigma$. At the beginning of a simulation, a list is constructed of all the neighbors of each molecule, for which the pair separation is with in $r_{list.}$ This is the first array and is called "list". Another list is an indexing array, "point". It points to the position in the array "list" where the first neighbor of molecule I+1, and the last neighbor I. "list(I+1)" points to the first neighbor of molecule I+1, "point(I+1)-1" points to the last neighbor of molecule I.

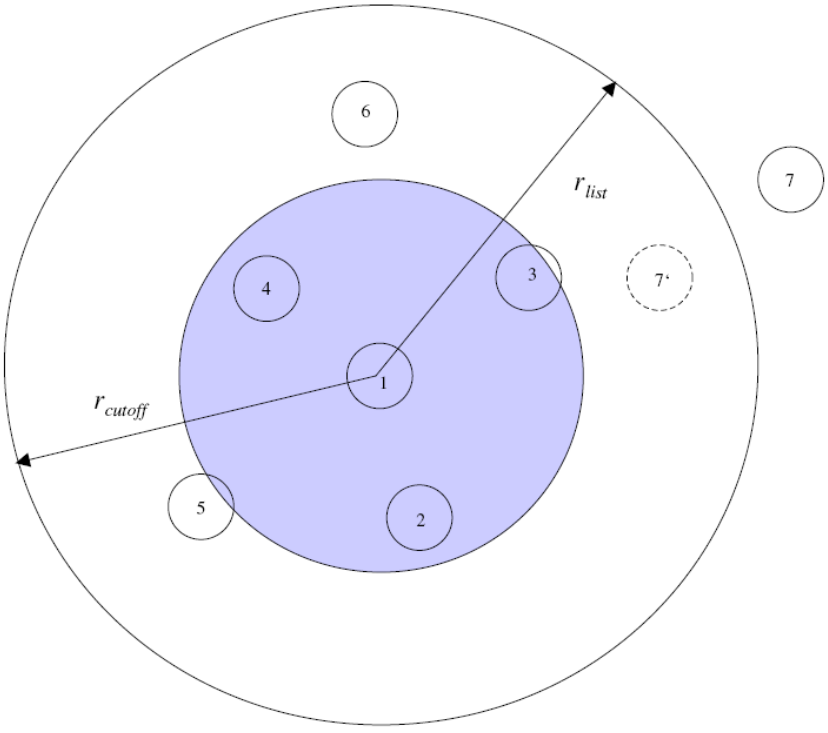

Figure 7 The cutoff sphere and its skin around a molecule

.

Take molecule 1 in the above picture for example. It will have molecule 2, 3, 4,5 and 6 in its LIST. However molecule 5 and 6 will not interact with 1 initially since they are out of the

cutoff distance. Molecule 7 is neither in the "list" or has interaction with molecule 1. However, several time steps later molecule 7 may enter molecule 1's "list" again and 5 or 6 may leave the "list".

The main advantage of this list is that we do not have to check if molecule 1 interacts with molecule 7, knowing that 7 is located outside of the list sphere for 1, and can not penetrate the "skin" that lies between list radius and the cutoff radius at the mean time. As the simulation proceeds, molecule 7 may enter the "skin", whenever 5 and 6 may leave it. We will simply update the list and again seek for interactions with 1 only among the molecules, staying inside its list sphere. The list needs to be updated from time to time. An interval of 10-20 steps is quite common. The rule of sum to update the list is when the sum of the magnitudes of two largest displacements of each molecule exceeds $r_{list} - r_{cut}$.

CHAPTER FOUR
MOLECULAR DYNAMICS SIMULATION PROGRAM

4.1 Initial Configuration Setup

The top and bottom walls are composed of 168 silicon atoms per layer oriented in the <1 1 1> direction. As it is shown in figure 7, the top and bottom walls are symmetric with respect to the middle line of the channel. Although the wall is considered interacting with the fluid, it is still assumed to be rigid for simplification in this simulation [43].

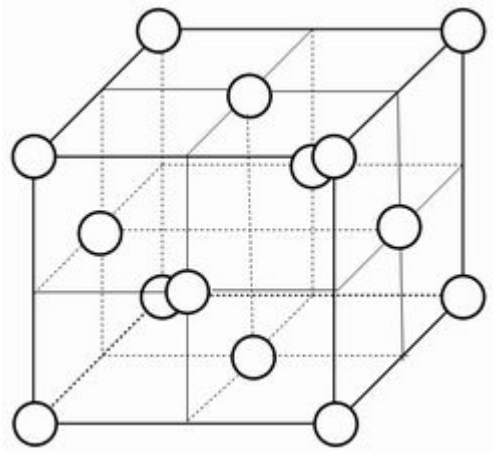

Figure 8 Unit cell of the F.C.C. for initial set-up for molecular dynamics simulation

(Picture courtesy Allen and Tildesley, 1987 [1])

The system schematic is shown in Figure 9. Each wall has four layers of silicon atoms. Channel length, width and height (L_x, L_y, L_z) are 4.588 nm, 4.588nm and 3.614nm respectively. There are 2048 liquid molecules which are sandwiched between top and bottom walls with a FCC structure as the initial configuration.

The SPC/E (extended simple point charge) model which was developed by Berendsen *et al* [1]. are a popular model that is being used in many molecular dynamics simulation group. SPC/E model considers the water molecule as a polar, hydrogen-bonded molecule with detailed molecular information. To track three times more particles can still be challenging today even though the computer memory and CPU speed has increased dramatically. In this study the water molecules are assumed to be spherical, nonpolar and neutral particles. This model was chosen for computational simplicity and to putatively examine the validity of continuum theory.

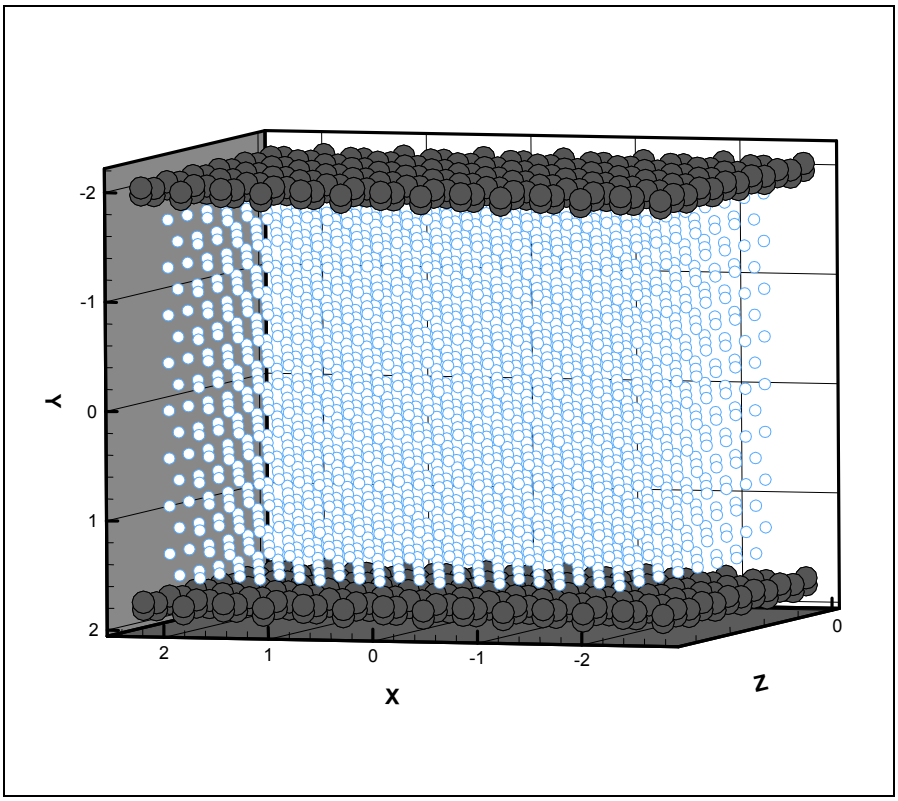

Figure 9 Simulated System Initial Configuration

For electroosmotic flow, 32 water molecules are randomly picked and converted to be chloride ions inside the channel by changing the molecule properties and adding a point charge

to each on of these 32 water molecules. The layers of the wall adjacent to the water are partially charged. 32 wall molecules out of each layer are randomly selected and assigned a positive charge. This was done due to the reason that flow is insensitive to the distribution of charges on the wall. For electroosmotic flow, there are 7 pairs of forces. Note that Ion-Ion and Ion-Wall interaction both have Lennard-Jones force and electrostatic force.

- Lennard-Jones forces: Water – Water, Water –Wall, Water – Ion, Ion – Ion, Ion – Wall
- Electrostatic forces: Ion– Ion, Ion – Wall

In order to increase the efficiency of the run, special attention were paid to the book keeping of the molecules, so that the loop will not go through every single molecule in the system. This was done by reorganizing the book keeping counter, so that from 1 to n-32 are water molecules, n-31 to n are ions, n to n+32 are charged wall molecules, n+32 to 1344 are neutral wall molecules.

4.2 Initial Velocity Assignment

In molecular dynamics simulation, an initial velocity is usually assigned to each molecule at the beginning to get rid of the initial configuration effect. The initial velocities are chosen randomly from a Gaussian distribution with the requirement of having the magnitudes meeting a specific temperature. The Boltzmann equation is used to calculate the velocities

$$\left(\vec{V}_i^{\,2}\right)^{\frac{1}{2}} = \left(\frac{3k_B T}{m_i}\right)^{\frac{1}{2}} \tag{4.1}$$

where k_B is the Boltzmann constant, m_i is the mass of each molecules or ions.

A Gaussian distribution was used to generate random numbers which were multiplied to the velocity from the Boltzmann equation. See appendix for detailed coefficients.

The rule of sum before proceeding to the main program is to remove the overall momentum due to the reason that there is no pressure gradient at the beginning of the run. So first the average particle velocity needs to be calculated by the following equation

$$\vec{V}_{ave} = \frac{\sum_{i=1}^{N} \vec{V}_i}{N} \tag{4.2}$$

where N is the number of fluid molecules in the system and V_i is the molecular velocity. Total momentum in the system is given as

$$\vec{P} = \sum_{i=1}^{N} m_i \vec{V}_i = m_i \vec{V}_{ave} \tag{4.3}$$

where m_i is the mass of each molecule. The total momentum will become zero when the average velocity is subtracted from each particle

$$\vec{P} = m_i \sum_{i=1}^{N} \left(\vec{V}_i - \vec{V}_{ave} \right) = 0 \tag{4.4}$$

whereas individual particle velocities will retain non-zero values.

4.3 Molecular Dynamics Simulation Program

The flow chart of the whole dynamic simulation program is presented in Appendix 4. The program starts by asking the user to define the total number of time steps. Then the program will construct the computational domain by creating the channel wall, liquid molecules as well as ions in FCC lattice. This was done to avoid initial overlaps within the system. Next initial velocities are assigned to each water molecules and ions based on Gaussian distribution. The final step for the initial setup of the program is to check if there is any initial overlap of particles due to system creation error.

By now, the program will go in to the main loop where the Lennard-Jones forces and electrostatic forces are calculated first. The forces on each particle are sent to the move subroutine where trajectories are calculated based on the Newton's second law. Since this simulation starts from a lattice at a different temperature, it is required to equilibrate for a number of time steps. We check the equilibration by monitoring the mean squared displacements of molecules from their initial lattice positions [1]. The criterion is to wait until the root-mean-squared displacement exceeds 0.5σ and it is clearly increasing. At the same time, all memory of the initial configuration will be erased. Once this is done, the external forces and thermostat is switch on and the results are counted towards the final results calculation. The periodic boundary condition is applied to all the fluid molecules and ions to ensure the number of density stays constant. Finally all the time dependent properties are sent to the averaging subroutine where the results are written out in the output files.

CHAPTER FIVE
RESULTS AND DISCUSSION

5.1 Pressure Driven Case Study

In order to have a better understanding of the nano-scale hydrodynamic behavior, we have performed a thorough molecular dynamics study on pressure driven flows. Three different types of case studies were conducted for pressure driven flow. They are:

a) Comparison study between continuum theory and molecular dynamics simulation results.

b) Parametric study of the effects of external force on the system.

c) Validity study of continuum theory by molecular dynamics method.

For most part, the standard Lennard-Jones reduced units which measure length in units of σ and energy in units of ε is used in this chapter. The unit conversion can be found in Appendix 3 at the end of the thesis. Note that the reduced unit carries an asterisk sign.

5.1.1 Comparison of Continuum Theory Prediction and Molecular Dynamics Result

In this study, the working fluid is liquid phase water (n*=0.8). Channel height is 11 σ. Simulation starts with both solid and fluid molecules distributed into face center cubic. Initial velocity based on a temperature of 300 K is randomly assigned to the fluid molecules. The fluid molecules are allowed a period to equilibrate in order to get rid of the starting structure and achieve the liquid water structure. This period is not ended until the root-mean-square displacement exceeds 0.5 σ, which usually takes about 2000 time steps. The external force is then

turned on after the system reaches its equilibrium. Then the thermostat with a time constant of 2×10^{-14} s is switched on to maintain the system temperature around 300K. The velocity and density results are averaged over 2 millions time steps.

Following is the equation used to calculate the continuum velocity from Navier-Stokes equation assuming the fluid is incompressible [42].

$$\vec{u}^* = \frac{\vec{F}_x^{\,*} n^*}{2\mu^*}\left[(h^*/2)^2 - (y^*)^2\right] \tag{5.1}$$

where $\vec{u}^*$ is reduced velocity, $\vec{F}_x^{\,*}$ is reduced force, n^* is number of density, μ^* is reduced viscosity, h^* is reduced channel height, y^* is the reduced location along channel height. The detailed unit conversion can be found in Appendix 3.

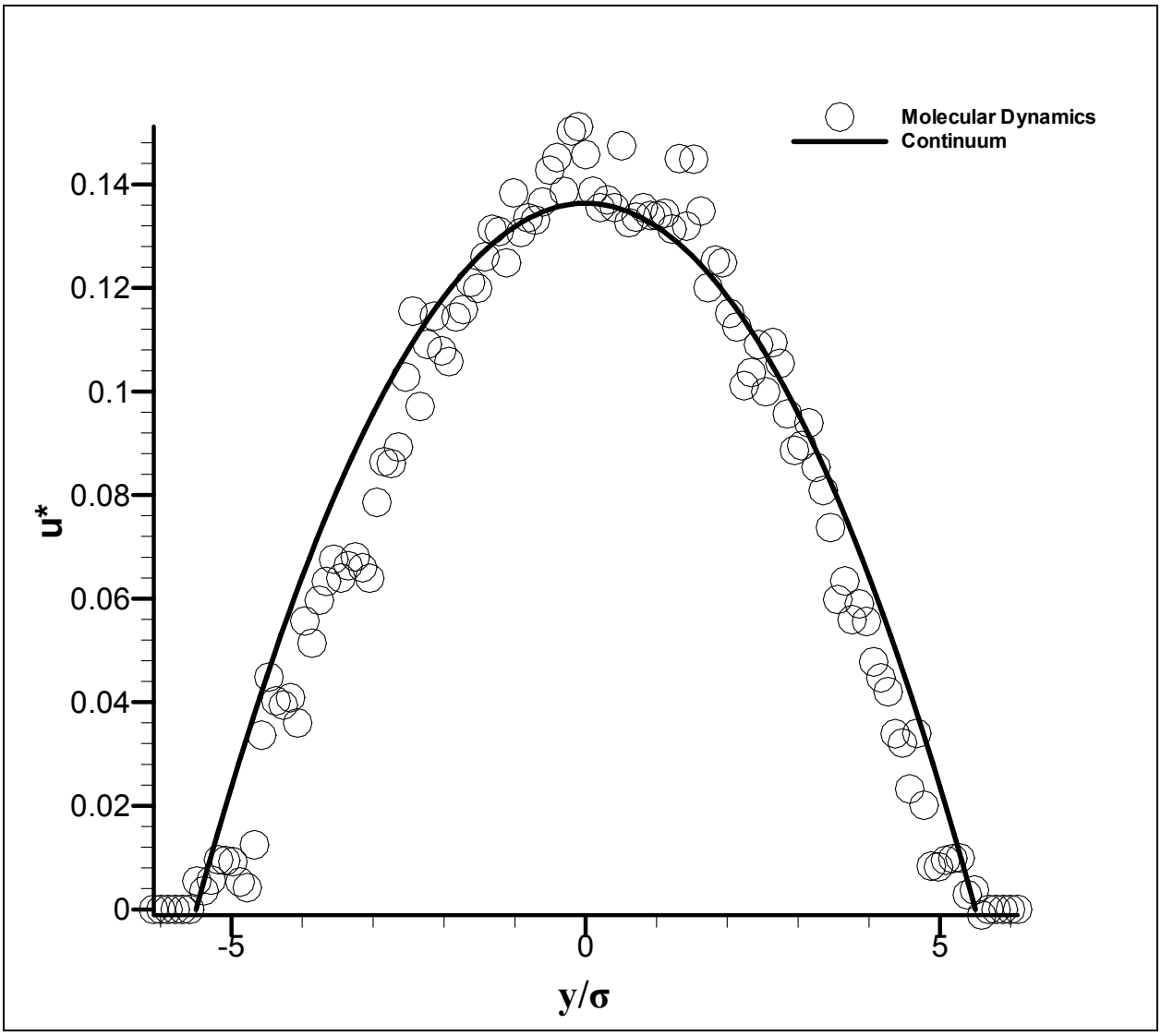

Figure 10 Comparison between MD and continuum results of pressure driven flow, Fe* = 0.024

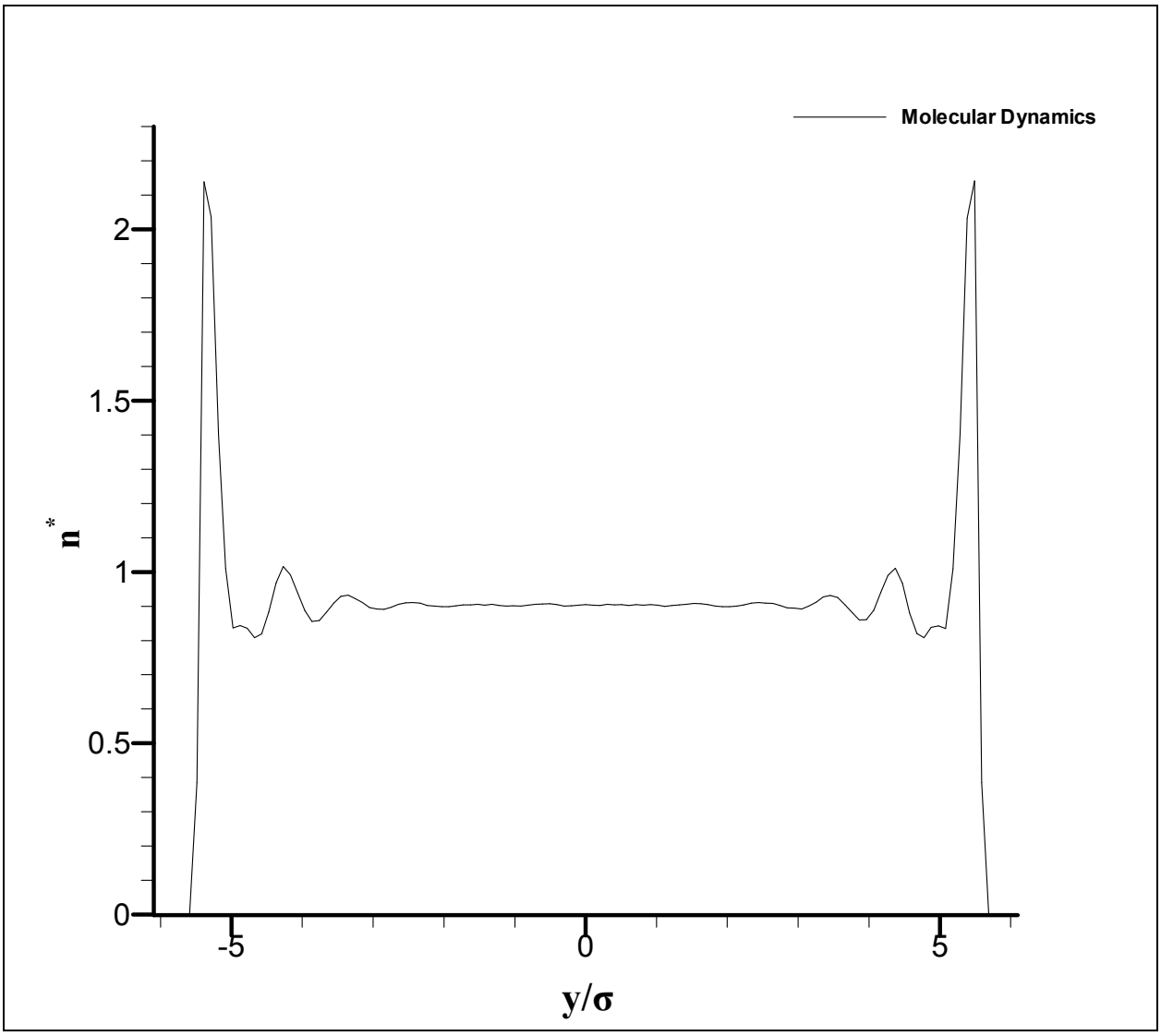

Figure 11 Pressure driven flow density distribution, Fe* = 0.024

Figure 9 shows the comparison between numerical results from molecular dynamics simulation and analytical results from equation (5.1). The magnitude of MD velocity profile and the theoretical results almost coincided. Even though the MD velocity profile appears to be parabolic shape, we can still see some small slips near the channel wall as Travis and Evans predicted. Slip boundary has been observed in a variety of simulations: "nonwetting fluids, fluids with weak interactions with walls, low-density fluids, molecular fluids, large shear rates, and fluid in which the corrugation length scale of the wall departs significantly from that of the fluid particles"[42]. In our case, the corrugation wavelength of the wall is the same as the fluid particle size and the interactions between fluid-wall interactions are similar to fluid-fluid particle interactions. Thus, it makes sense that we see insignificant slip at the wall. We can conclude that continuum theory can adequately describe the simple pressure driven flow through channel height at $h/\sigma = 11$ [42].

It is worthwhile to notice that the density at this channel height completely deviate from continuum theory where uniform density is assumed cross the channel height [45]. We can see zero density about $h/\sigma=0.5$ away from the channel wall, two spikes next too it and small oscillation in the close to wall vicinity. The density distribution is fairly uniform the middle part of the channel. The reason that there is no molecules within $h/\sigma=0.5$ from the wall is because molecule's physical boundaries and the repulsion force between molecules. Such a density profile has been confirmed by Travis *et al.* and other researchers as well [11,12,13,42]. This agrees with their conclusion that classic continuum theory breaks down in the region near the wall when the state variable such as density and temperature is not constant.

5.1.2 Parametric Study of the Effects of External Force on the System

In this section we will discuss the parametric study where the effects of external forces was looked into. The following table illustrates the four different cases in which we analyzed the effects of external force on the pressure driven flow system. Note that the system configuration and other properties are kept the same for all four cases. The objective of this study is to investigate solely the influence of external force on velocity profile in the same system.

Table 2 Parametric Study of Pressure Driven Flow

	External Force* Fe_x*	**h***	**n***
Case 1	0.024	11.0	0.87
Case 2	0.05	11.0	0.87
Case 3	0.1	11.0	0.87
Case 4	0.15	11.0	0.87

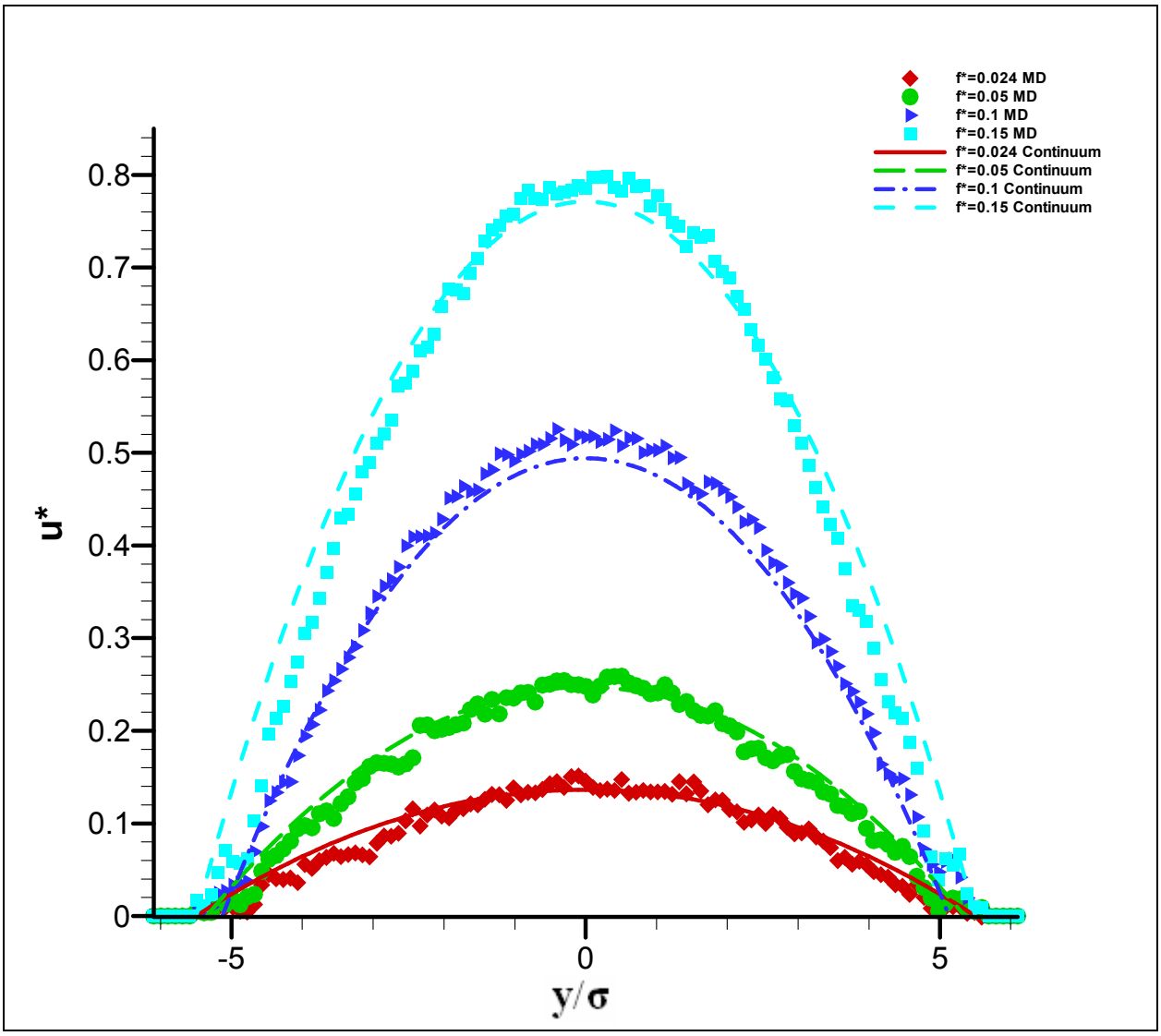

Figure 12 Pressure driven flow velocity profiles under various external forces

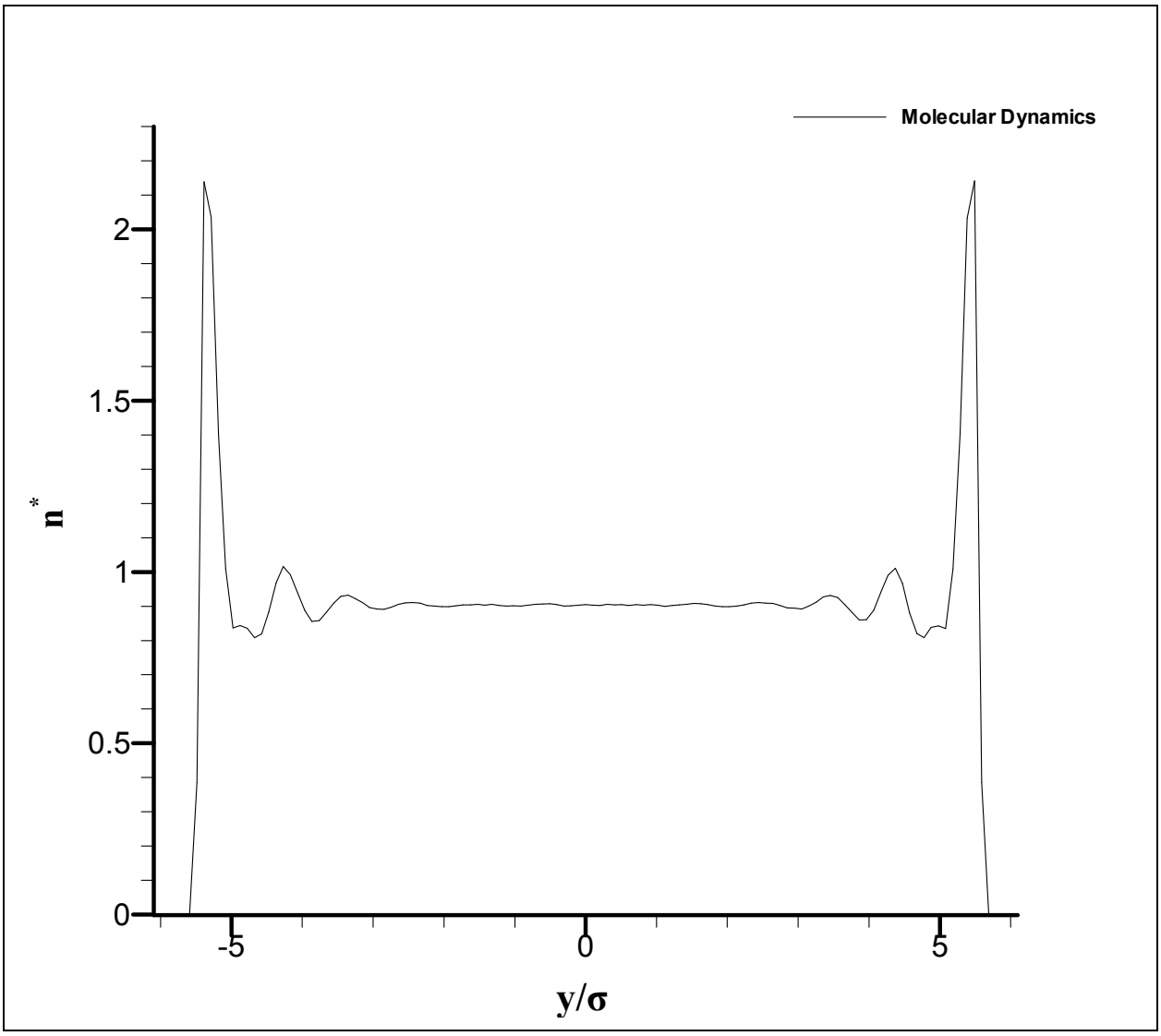

Figure 13 Pressure driven flow density distributions under various external forces

The velocity fields of case 1 to 4 are summarized in figure 12. As expected, all the velocity fields are parabolic like. Case 4 which has a non-dimensional external force is 0.15 has the highest magnitude and the case 1 with external force of 0.024 has the smallest one. It is obvious to see that the magnitude of the velocity profile is proportional to the external force magnitude. This agrees with the 1-D incompressible Navier-Stokes equation, where it states that the velocity fields should be parabolic shape and the magnitude of the field is proportional to the external pressure field intensity. Despite the layering of fluid near the wall, continuum theory provides a quantitative description of the velocity profile.

We also discovered that molecular dynamics results look smoother when the external force is higher. The reason is due to that the system has overcome more thermo noise when external force is higher.

All the density distributions are very identical due to the reason that the densities in all cases are kept the same. It can also be concluded that density fields is independent of velocity magnitude in the system.

5.1.3 Validity Study of Continuum Theory by Molecular Dynamics Method

Even though we did see some degrees of mismatch between continuum theory and MD results in the previous studies with a channel height more than 10σ, continuum theory still provides adequate understanding of hydrodynamics in nano channels. The third study was designed based on the objective to find the limit of the channel height when the velocity profile does not look parabolic any more, that is when the Navier-Stokes equation completely fails.

Travis and Gubbins reported that the velocity field and density distribution would look very distinct from the continuum theory when the channel height is around 5σ. We have decided to build the model with a channel height of 5.5σ in order to compare the results with existing literatures. The working fluid is kept as liquid phase water (n*=0.8). Simulation starts with both solid and fluid molecules distributed into face center cubic. Initial velocity based on a temperature of 300 K is randomly assigned to the fluid molecules. Then the thermostat with a time constant of 2×10^{-14} s is switched on to maintain the system temperature around 300K. Due to the reason that the channel height is much smaller than the previous run, we averaged the results over 3 millions time steps. The external force used is 0.1, which is comparable to case 3 in the parametric study.

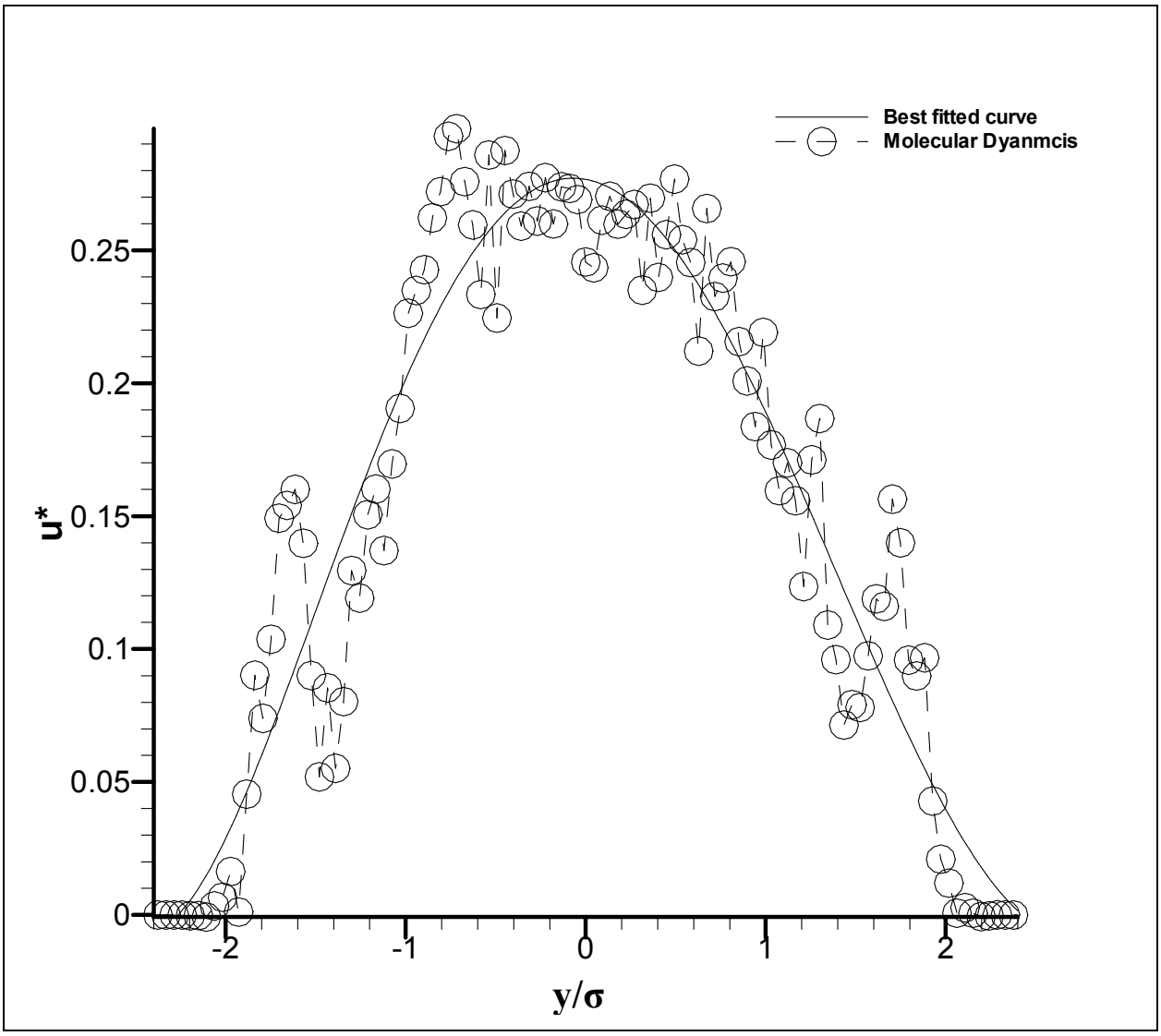

Figure 14 Pressure driven flow velocity profile with channel height of $h/\sigma = 5.5$

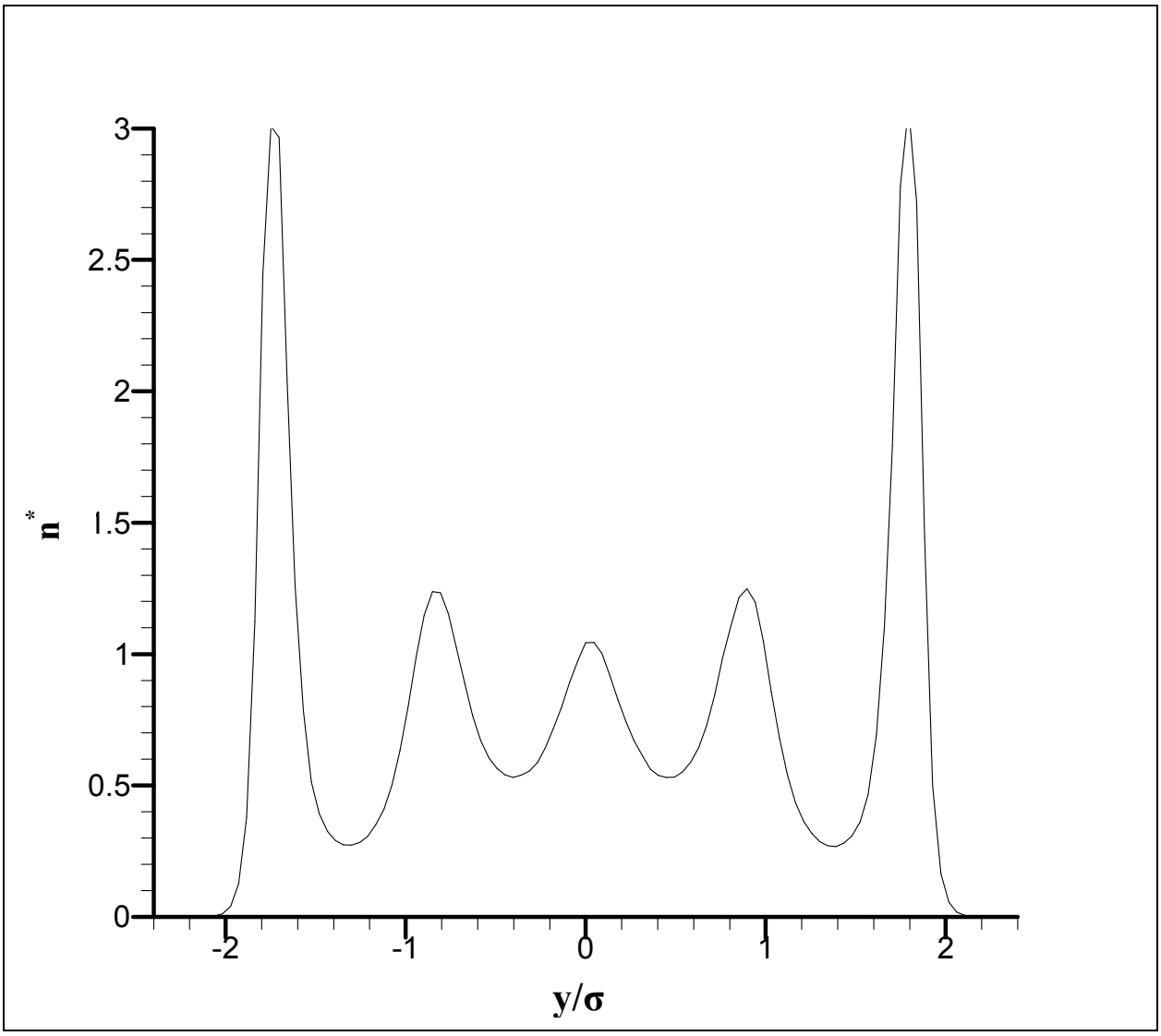

Figure 15 Pressure driven flow density distribution with channel height of $h/\sigma = 5.5$

When the channel height is only $h/\sigma=5.5$, the velocity profile from the molecular dynamics simulation shows a bell-like shape that has two big jumps near the wall. Figure 13 illustrates the velocity field of this case. The solid line is the 4^{th} order best fitted curve. Such a behavior of fluid is induced by the high strength of the wall-fluid interaction. This can be easily understood because the fluid experiences a greater opportunity of interacting with wall than in previous study when the channel height is $h/\sigma=11$.

The density profile does not look the same as $h/\sigma=11$channel height cases either. We no longer see the uniform density in the middle of the channel; rather we saw three peaks throughout the channel height. This agrees with what Travis and Gubbins showed in his paper [14]. Figure 16 shows the density profiles from their paper. This result gives sufficient evidence that Navier-Stokes equation breaks down when the channel height is around five molecular diameters.

5.2 Electroosmotic Flow Case Study

Electroosmotic flow is the core study of this research. In this study, we primarily studied three different phenomena of this particular flow.

a. Qualitative comparison with continuum results

b. Parametric study of effect of external electric field on flow magnitude

c. Parametric study of different density system

In order to enhance the signal-to-noise ratio, the external field strength is chosen to be greater than the real experiment value. Due to the low density of ions in our system, the simulation is generally run over a long period to get reliable statistics. Usually 2 millions time steps is required in electroosmotic flow simulations.

5.2.1 Comparison of Continuum Theory Prediction and Molecular Dynamics Result

In the molecular dynamic part of the study, the working fluid is still liquid phase water ($n^*=0.8$). Channel height is kept as $h/\sigma=11$. Ions are introduced in to the system in order to generate the electroosmotic flow. Please see chapter 2 for details regarding to the electrokinetic interaction modeling. Simulation starts with wall and fluid (water molecules and ions) distributed into face center cubic. Initial velocity based on a temperature of 300 K is randomly assigned to the all the fluid molecules and ions.

On the other hand, for continuum theory, we decided to use the methodology Burgreen and Nachache developed [24]. They were the first people tried to solve the ion concentration and electrokinetic flow problem in nano channels analytically. Other research groups [26,42] have also tried to do the same job by substituting the ion concentration obtained from the MD

simulation into the Navier-Stokes equation to come up with the velocity profile across the channel. This method was not preferred because by using results from numerical simulation could have introduced numerical error to analytical results. The analytical results thus become hard to justify.

Assuming that we are dealing with a simple electrolyte, which ionized into two equally charged ions of valence z, the net charge per unit volume,

$$\tilde{\rho} = \bar{n}ez(e^{\alpha\psi/\psi_0} - e^{-\alpha\psi/\psi_0}) = -2\bar{n}ez\sinh(\beta\psi/\psi_0) \tag{5.3}$$

where $\beta = ez\psi_0 / kT$.

We can link the charge density and potential by the one dimensional Poisson equation,

$$\frac{d^2\psi}{dy^2} = -\frac{4\pi}{D}\tilde{\rho} \tag{5.4}$$

After plugging in the net charge density, Poisson equation will have a final form of

$$(\omega\eta) = \omega(h-y) = \int_{\psi}^{\psi=\psi_0} \frac{d(\beta\psi/2\psi_0)}{\left(\cosh^2\frac{\beta\psi}{2\psi_0} - \cosh^2\frac{\beta\psi_c}{2\psi_0}\right)^{1/2}} = \kappa\left[F(\frac{\pi}{2},\kappa) - F(\theta_0,\kappa)\right] \tag{5.5}$$

where $F(\theta,\kappa)$ is called the elliptic integral of the first kind,

$$\theta = \sin^{-1}[\frac{\cosh(\beta\psi_c/2\psi_0)}{\cosh(\beta\psi/2\psi_0)})]^{-1} \tag{5.6}$$

$$\theta_0 = \sin^{-1}[\frac{\cosh(\beta\psi_c / 2\psi_0)}{\cosh(\beta/2)})]^{-1} \tag{5.7}$$

$$\kappa = [\cosh(\beta\psi_c / 2\psi_0)]^{-1} \tag{5.8}$$

Figure 15 shows the variation of potential with respect to the channel height for β=4 case.

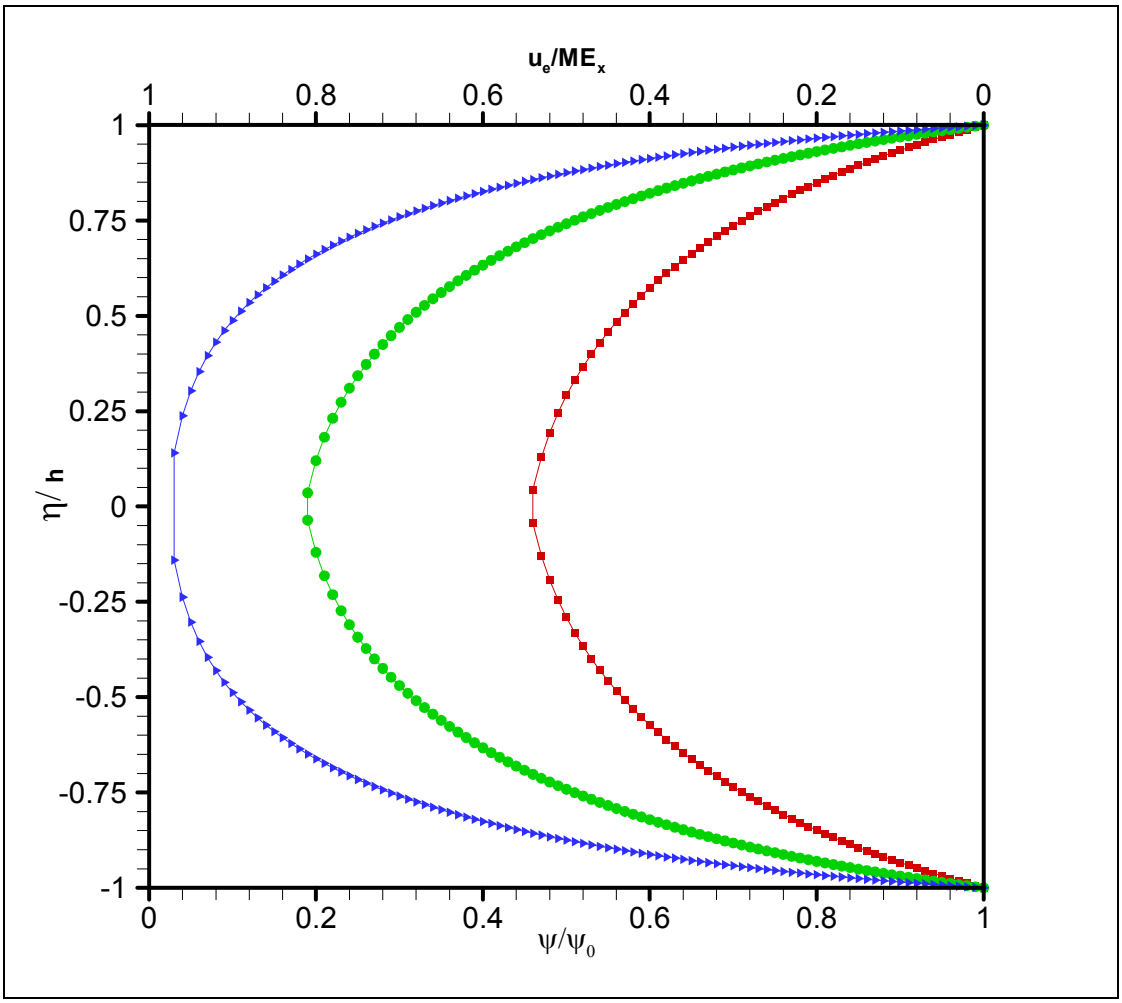

Figure 16 Variation of potential and electrokinetic β=4

If the external body force is only electric force, then Nervier Stokes equation becomes

$$\mu \frac{d^2u}{dy^2} + \frac{DE_x}{4\pi} \frac{d^2\psi}{dy^2} = 0 \tag{5.9}$$

where E_x is electric field.

After double integration and applying boundary conditions:

at surface u=0 and $\psi = \psi_0$; at channel center $du/dy = d\psi/dy$,

the relationship between velocity and ψ/ψ_0 is simplified as below

$$u = ME_x(1 - \frac{\psi}{\psi_0}) \tag{5.10}$$

where M is mobility. Figure 15 shows the analytical electroosmotic velocity.

In order to compare with the molecular dynamics results, we first calculated mobility by dividing the maximum MD velocity by maximum value of u/ME_x from figure 16. β=4, ωh=1 case was chosen because they are the closest to realistic experiment properties of nano channels. Non-dimensional Electric field E^*_x= 5. A mobility of 3.33×10^{-3} was found for this case. This mobility falls in the same range of values from MD simulation and experiments.

After dividing the MD velocity profile by ME_x, we found the following comparison between MD simulation results and analytical results.

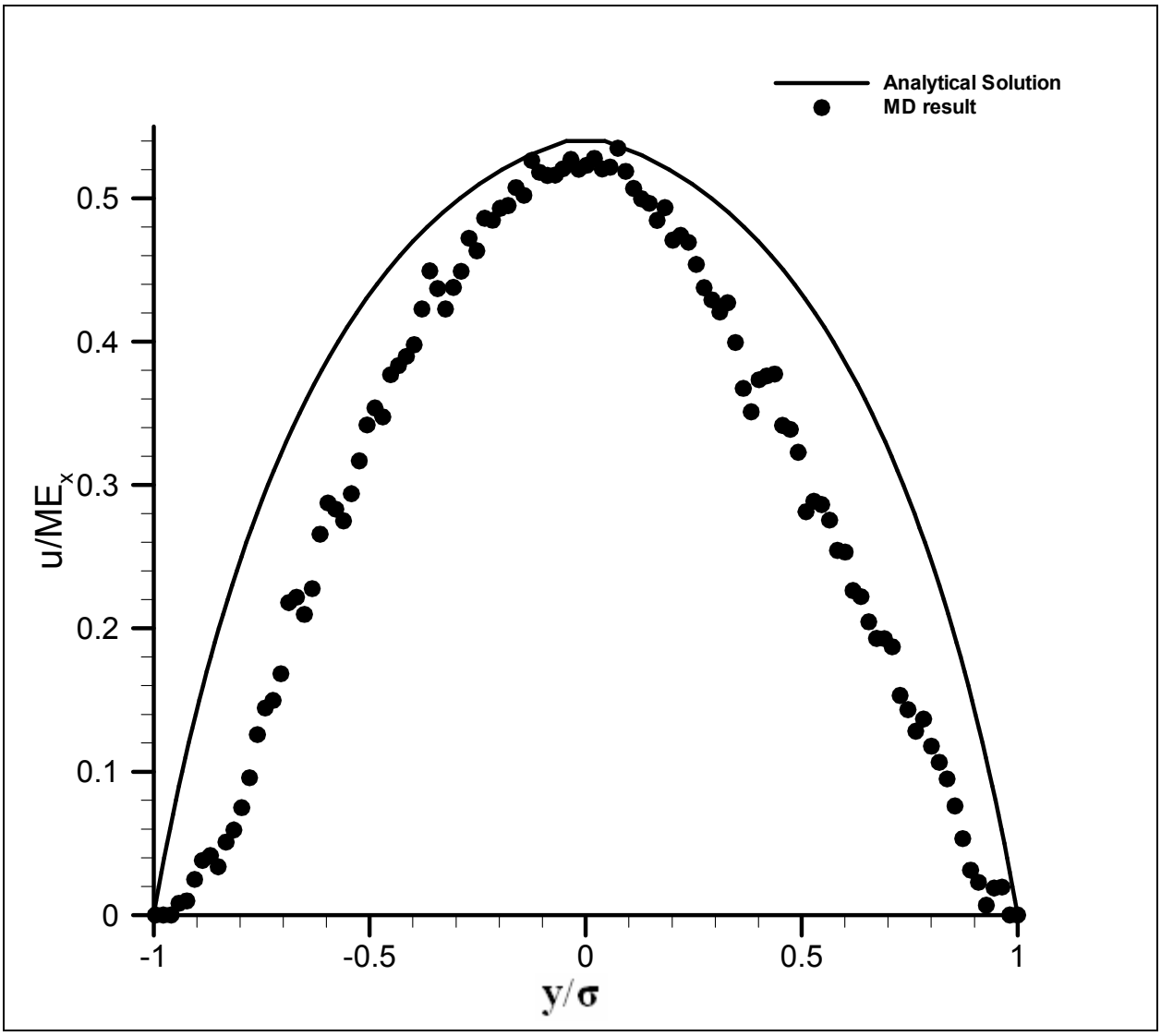

Figure 17 Comparison between MD and continuum results of electroosmotic flow, $E^*_x = 5$

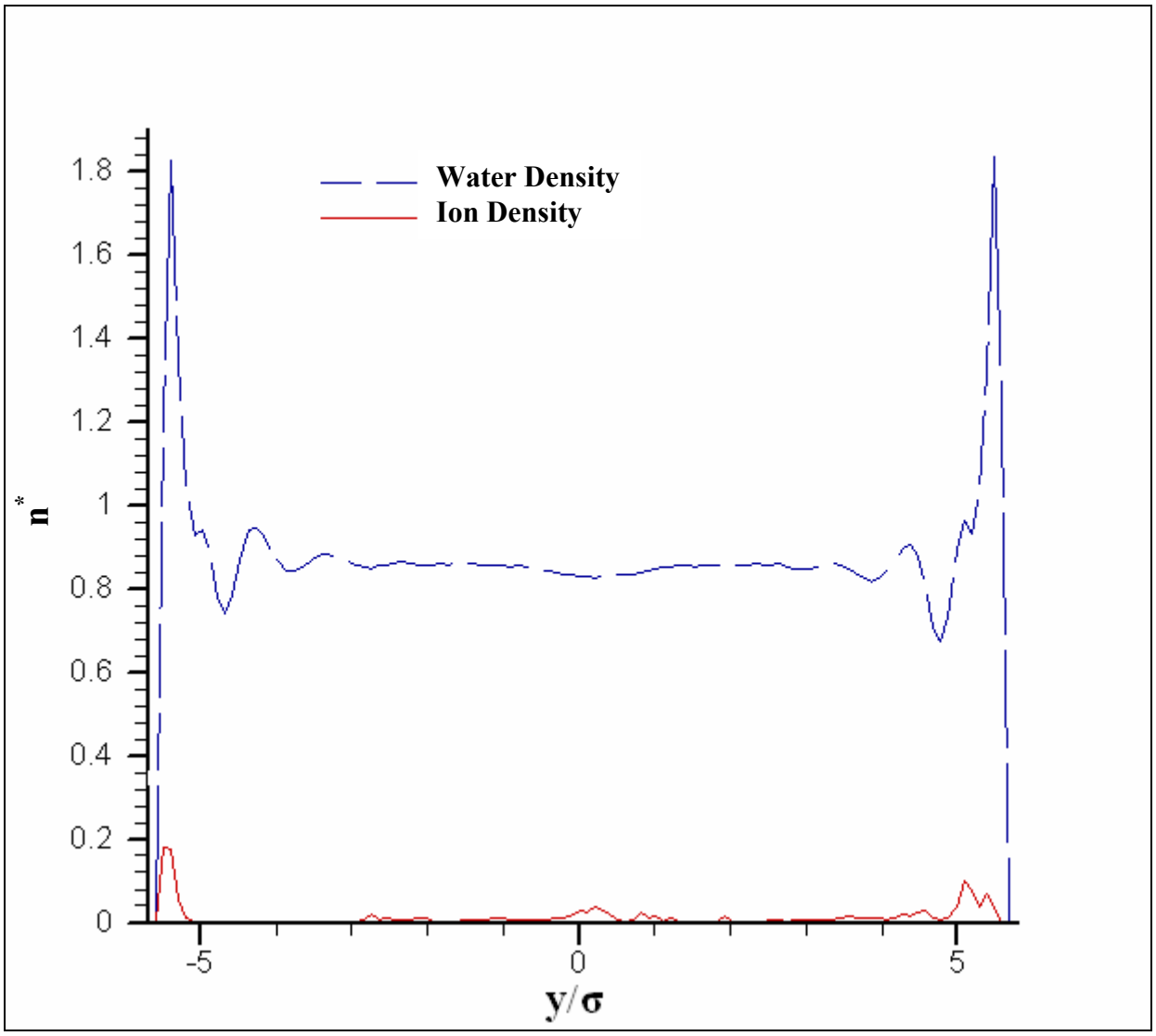

Figure 18 Electroosmotic flow water and ion density distribution, $E^*_x = 5$

Figure 17 shows the velocity profile from molecular dynamics simulation, which is compared with the continuum results calculated by Burgreen and Nachache's method. It can be seen that the continuum results have a wider parabola than the one from MD. The wider parabola could be caused by the wall effects that continuum theory fails to detail. In nano channels, we do see layers of water molecules accumulated near the wall. This might have caused the smaller velocity at near wall vicinity. However, they both have a parabolic shape as predicted in nano channel electroosmotic flow.

The parabolic shape of the velocity profiles is no surprise to us. In micro scale electroosmotic flow system, the channel height is generally much larger than the Debye length of the electrolyte, which is on the order of several nano meters. Since Electrokinetic effects are confined in the small region close to the wall, only the molecules in that region will be affected. On the other hand, when the channel height is only several nano meters, the double layers could be overlapping and the whole channel will be affected this time. Thus the velocity profile appears to be parabolic like.

As expected the water density looks different from the continuum theory's prediction, where we no longer see the uniform water density throughout the whole channel, but two peaks near the wall. The water density is very similar to what we saw in the pressure driven cases. The ion density distribution looks different from what it was expected from Poisson-Boltzmann equation as it ignores the molecular aspects of ion-wall and ion-solvent interactions. Once again, we found that the continuum theory fails to describe the area close to the channel wall at the nano scale.

5.2.2 Parametric Study of the Effects of External Force on the System

Table 3 lists the three different cases that were investigated in this parametric study. Each electroosmotic flow run is averaged over 2 million time steps. All the parameters used were listed in Chapter 2, where the Ewald summation governing equations and program were explained. The systems have the same channel height of $h/\sigma=11$. The three cases have the same water density, but increasing external electric field. The exact same MD program is used in all three cases.

Table 3 Parametric Study of Electroosmotic Flow

	External Electric Field*	**h***	**n***
Case 1	0.1	11.0	0.83
Case 2	0.5	11.0	0.83
Case 3	5.0	11.0	0.83

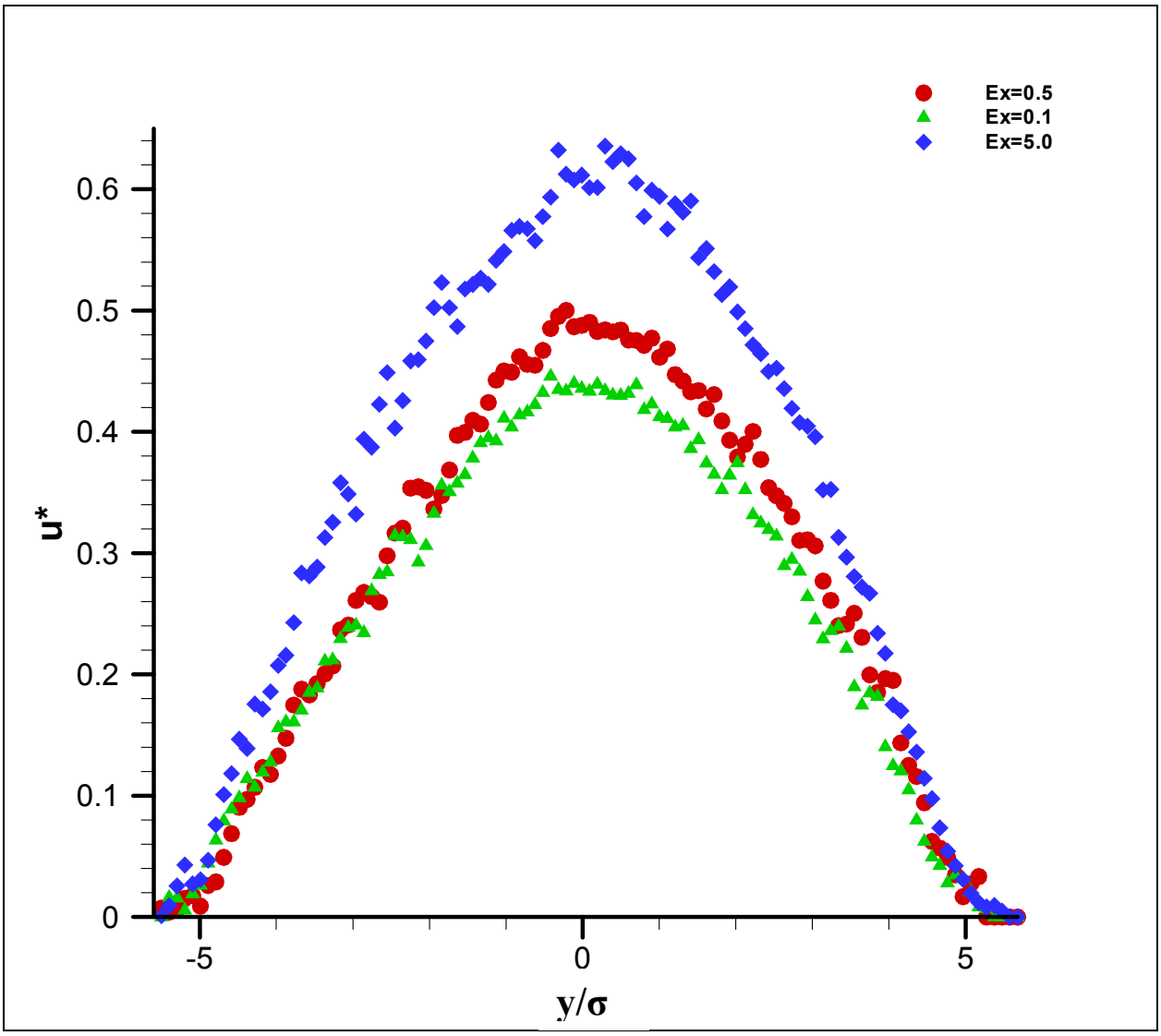

Figure 19 Electroosmotic flow velocity profiles under various external electric fields

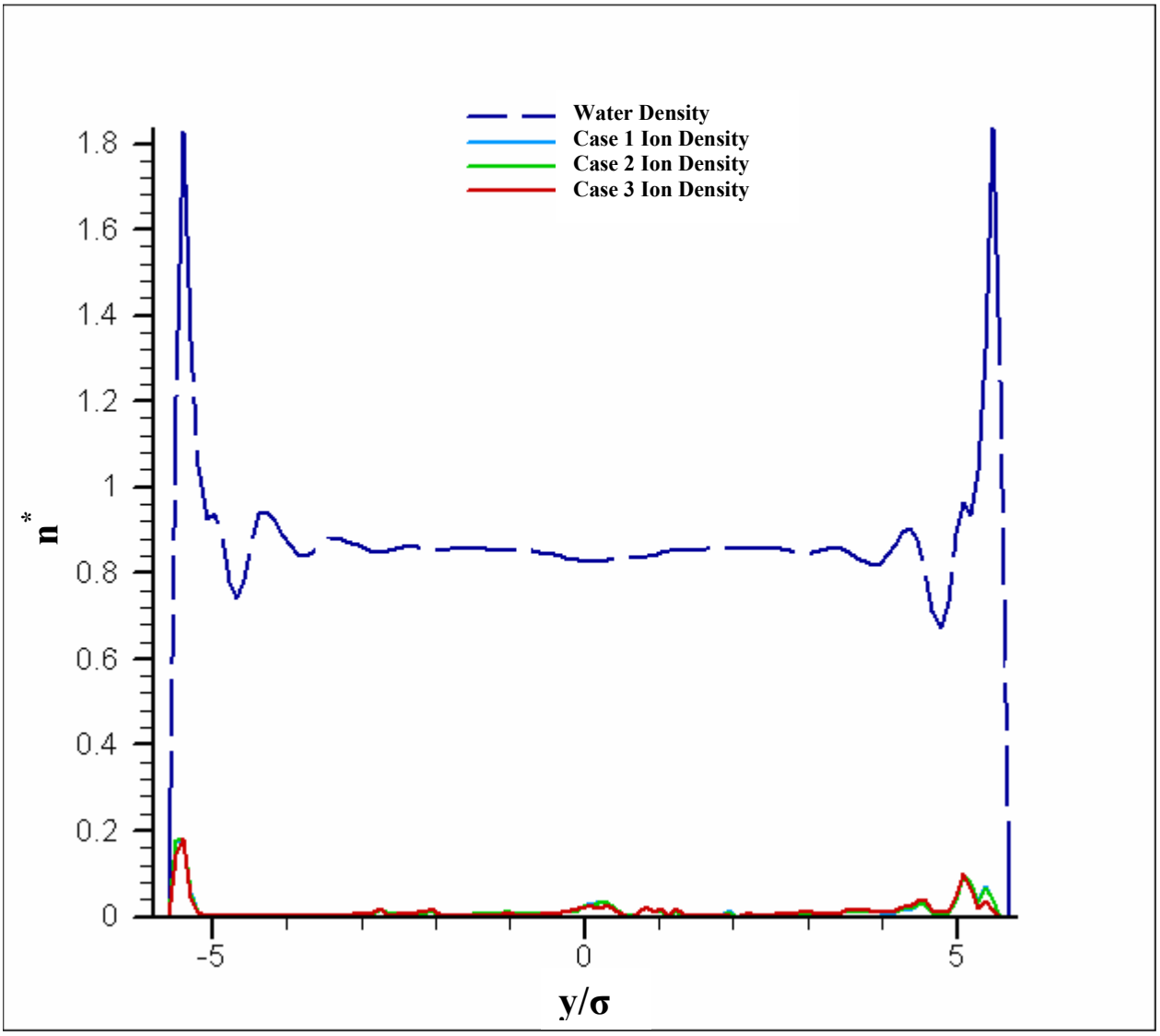

Figure 20 Electroosmotic flow water and ion density distribution under various external electric fields

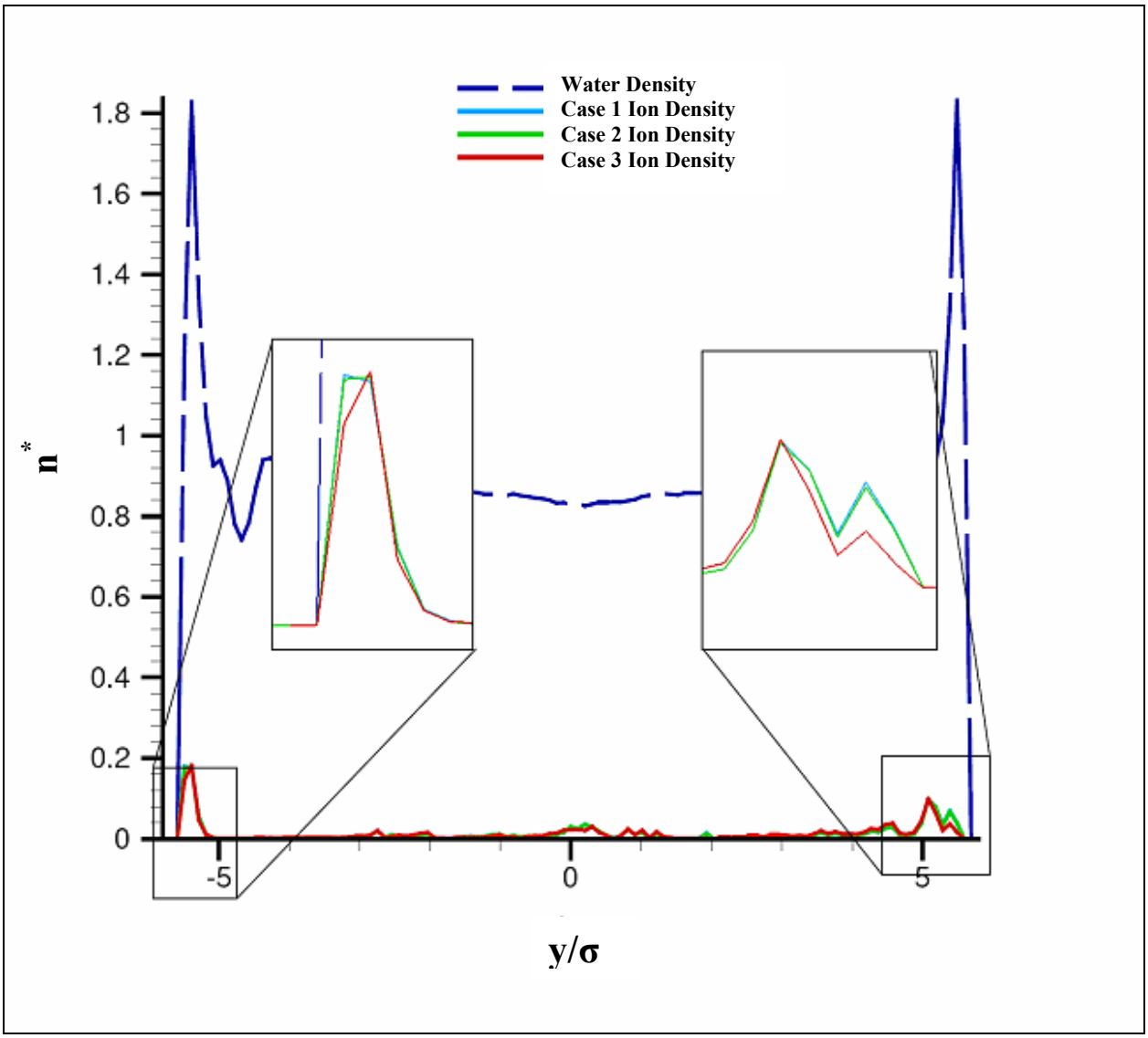

Figure 21 Details of electroosmotic flow water and ion density distribution under various external electric fields.

Having the same channel height and density, the magnitude of velocity profiles from MD simulation increases proportionally to electric field strength. This agrees with what the Navier-Stokes equation predicted

$$u = ME_x(1 - \frac{\psi}{\psi_0}) \tag{5.11}$$

Small degree of slip boundary is observed near wall. Such a behavior is the same as the continuum theory. By now, we can conclude that molecular dynamics simulation provides fairly adequate description of hydrodynamics behavior in nano channels at channel height more than $h/\sigma=10$. However, efforts need to be spent at analyzing the close to wall vicinity where slip boundary occurs and laying effects of water molecules occurs.

The water density profiles of three cases are coinciding together, whereas the ion density profiles vary slightly. Figure 21 has the zoomed in pictures of close to wall ion density distribution. The ion density is not fully symmetric. Unlike the left peak, which has ions attracted at a more focused area, the right side of the channel seems to have ions appearing more spread out. This can be explained due to the reason that our system is too diluted. Since we only have 32 ions in total, it would be difficult to have a perfectly symmetric distribution.

5.2.3 Parametric Study of the Effects of External Force on different density system

Table 4 Sensitivity case of Electroosmotic Flow

	External Electric Field*	h*	n*
Case 4	0.5	11.0	0.98

People have reported sensitivity to number of density in the system in pressure driven before. In electroosmotic flow we are also interested in the number density distribution sensitivity to hydrodynamics behavior. A number of density close to 1.00 was selected for this case. The same channel height, but slightly smaller channel length and width (x and z direction unit box length) were used in order to achieve greater water density. A comparable external electric field 0.5 is selected to keep the analyses simple. The same molecular dynamics program is used and the same time steps are achieved.

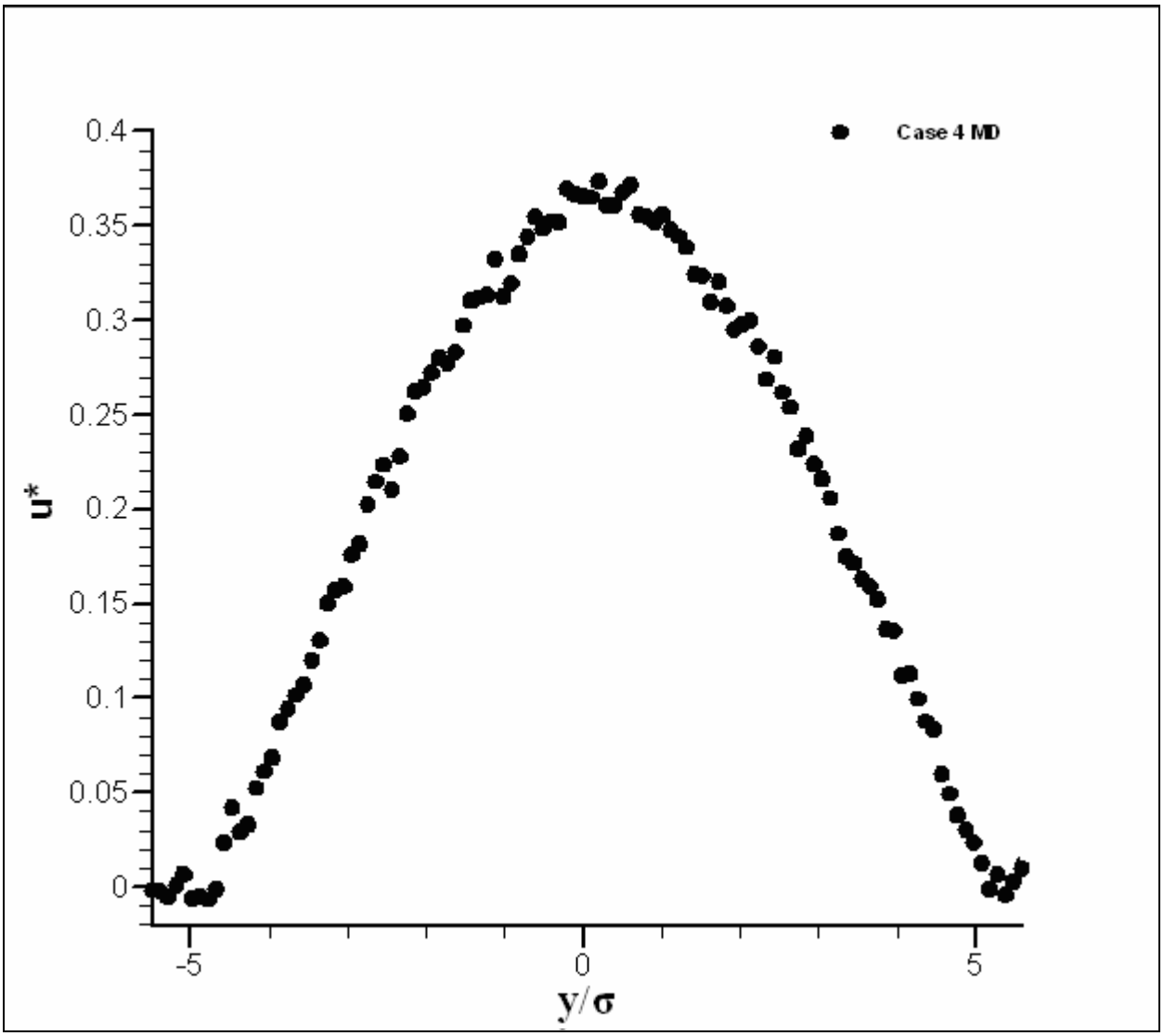

Figure 22 Electroosmotic flow velocity profile, n^*=0.98, E^*_x = 0.5

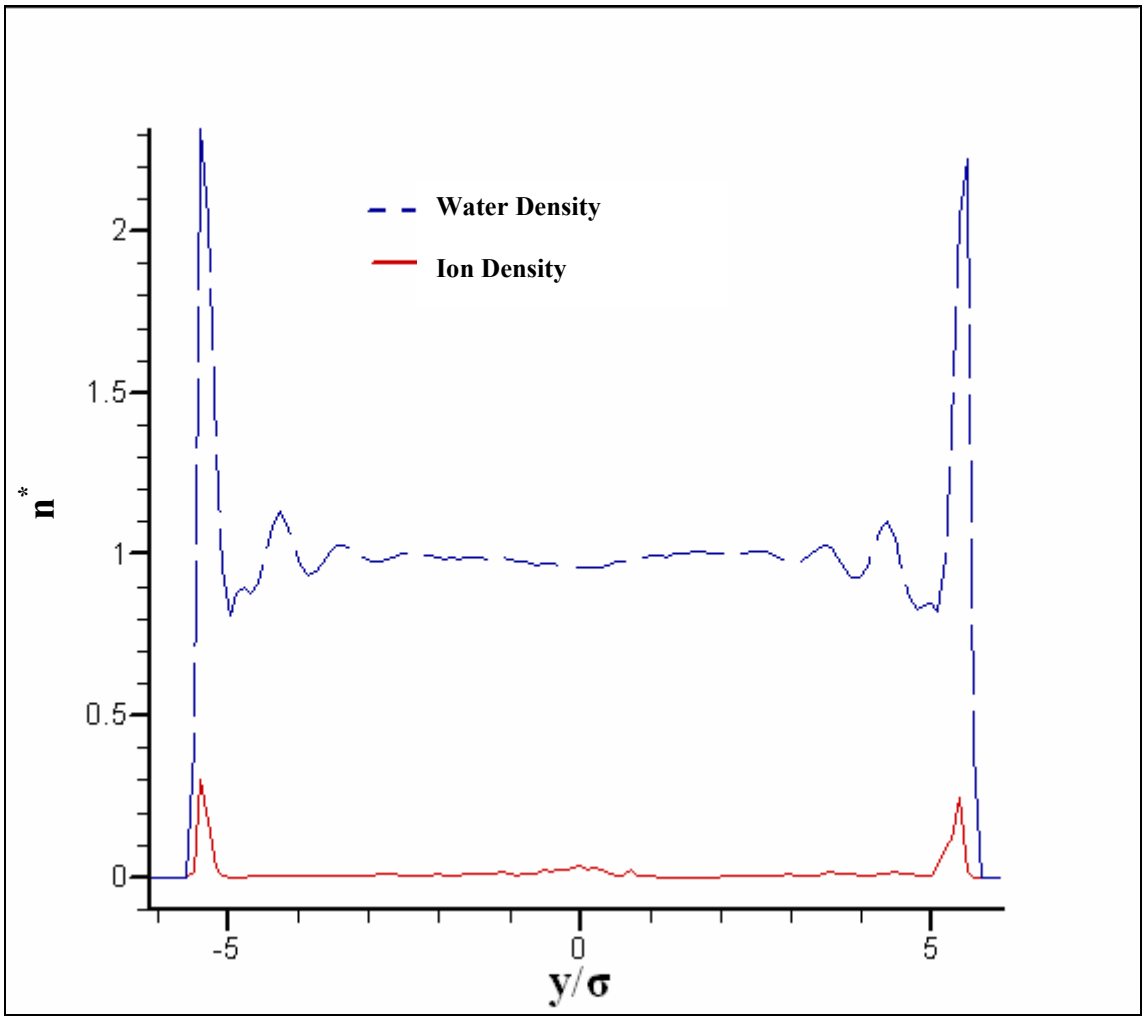

Figure 23 Electroosmotic flow water and ion density distribution, n^*=0.98, E^*_x = 0.5

Figure 22 shows the velocity profile of case 4. Once again, we observe parabolic shape of velocity profile. Compared to case 1 which has the same external electric field, the magnitude of the velocity is smaller due to the fact that this density is denser than the first case. At the wall, we are seeing small slip, which agrees with what we saw in the above cases. We can see that in this case, multi scale analysis may become a good approach in predicting the details near the wall and quickly knowing the velocity profile in the middle of the channel.

In figure 23, the water and ion density distributions of case 4 are presented. As far as the water density field, the shape looks similar to the system with smaller density. The density in the middle of the channel is increased obviously due to the increase of the whole system density. The density profile is showing the laying effects like pressure driven flow, which has also been confirmed by other research groups too [42]. What really different from the previous cases is the ion concentration, which seems a lot more symmetric than all the cases with smaller density. The high density of the system may have caused this interesting phenomenon. This can be caused due to the reason that in a more condensed system, the interaction between the wall molecules and ions are more likely to happen.

5.3 Energy Conservation

Energy conservation is a very important scale to evaluate the validity of the molecular dynamic simulation. The potential energy and kinetic energy of the system are given by

$$PE = \sum V_{f-f} + \sum V_{s-f} \tag{5.12}$$

$$KE = \sum \frac{1}{2} m_i \vec{V}(t)^2 \tag{5.13}$$

The total energy of the system should remain to be constant throughout the simulation.

$$U = PE + KE = const \tag{5.14}$$

However, as it was discussed in the second chapter, the potential energy and kinetic energy are not computed at the same time step. The kinetic energy is calculated at the mid step based on the previous mid step velocity and the acceleration, whereas the potential energy done at a full time step. We could do this because the time step is on the order of $\sim 10^{-15}$ s. So it is not fully correct to sum up these two types of energies and check the conservation. The following two figures show the change of kinetic energy and potential energy over a time step of 1 million respectively. As it shows the changes vary with in a range of ± 5% and ± 2% for kinetic energy and potential energy respectively. It can be concluded that the simulation is valid energy conservation wise.

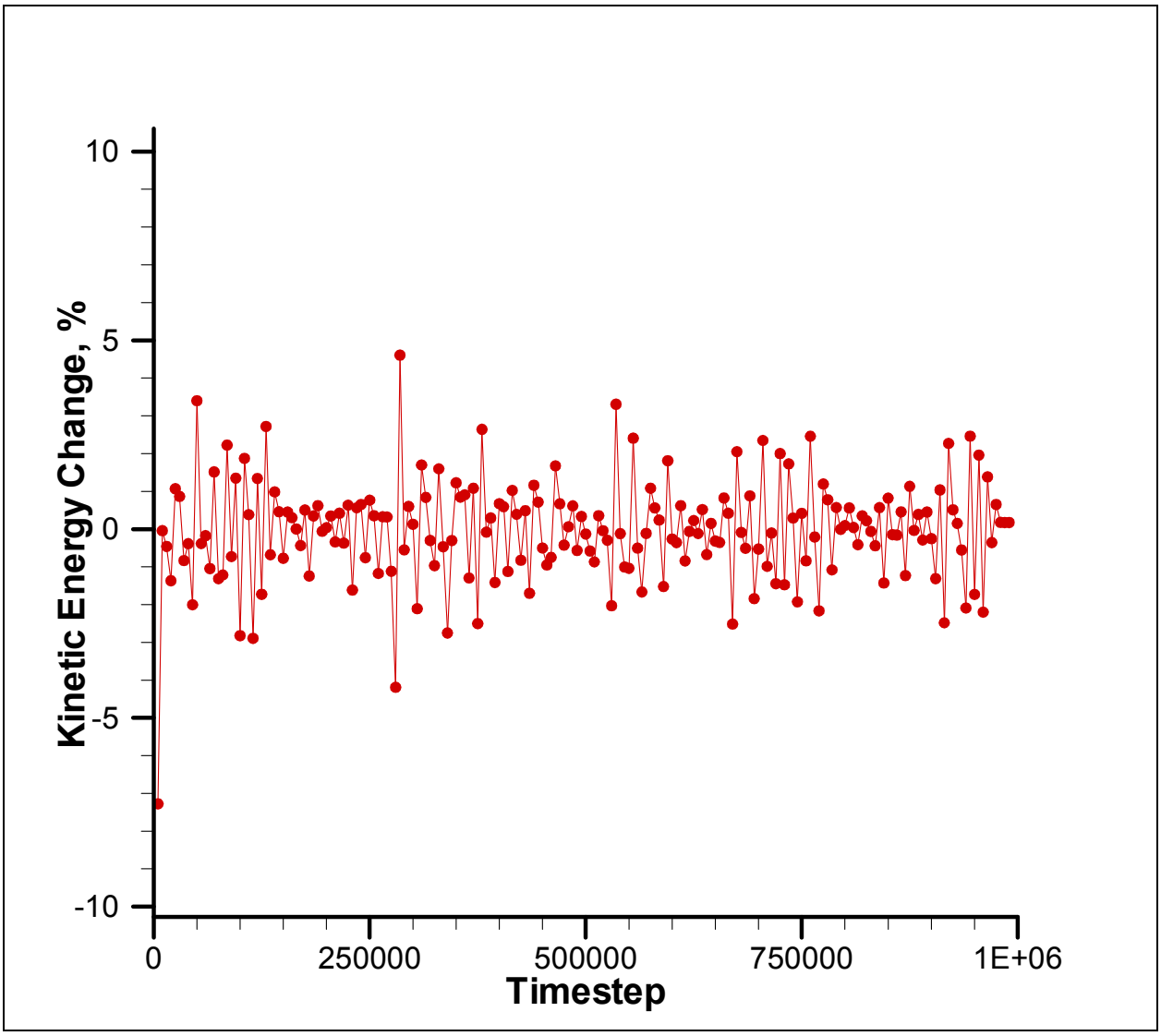

Figure 24 Kinetic energy change with regards to time over 1 million time steps

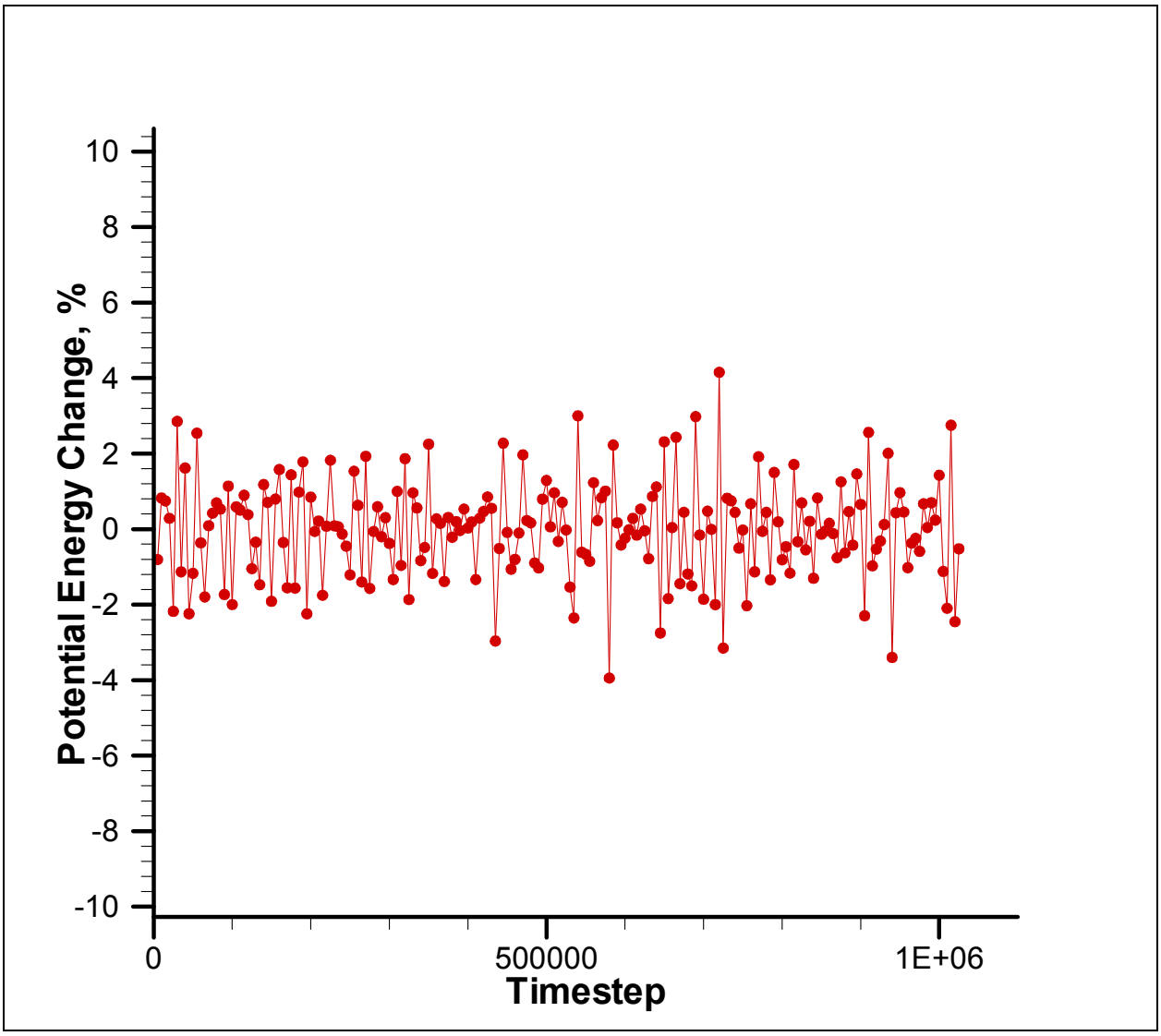

Figure 25 Potential energy change with regards to time over 1 million time steps

CHAPTER SIX
CONCLUSION

A molecular dynamics simulation was developed to simulate pressure driven flow and electroosmotic flow in nano channels. Two systems were developed. One is with pure water molecules and stationary walls. The other is composed of pure water, ions and charge walls. Lennard Jones potential was used as the van der Waals interaction. Ewald 3D corrector was applied to capture the electrostatic interaction. Periodic boundary condition was applied to simulate bulk flow and a Berendsen thermostat was used to control the system temperature.

For pressure driven flow, we have studied the flow behavior with respect to the external pressure gradient and compare the MD flow with the continuum velocity and density distribution. We found that continuum theory can adequately describe hydrodynamic behavior of pressure driven flow in channel with height of 10 molecular diameters We have also studied the fluid behavior in an ultra thin channel to discovered that in a channel height less than 5 molecular diameters, the continuum theory breaks down.

In the electroosmotic flow study, we have done a comparison study between analytical solution and MD simulation and a parametric study to investigate the effect of external electric field. Electroosmotic flow velocity is parabolic in channel of 11 molecular diameters. We have also studied the water and ion density distribution in a nano channel in normal density system and a denser system. Like pressure driven flow, velocity profiles of electroosmotic flow increase proportionally to the strength of external force

The future work should be focused on electroosmotic flow and mix of pressure driven and electroosmotic flow. With the help of super computer, we should significantly increase the number of ions in the channel. We should also consider introducing ions in our system to make the simulation more similar to a real ionized liquid. If allowed, water molecule's detailed

structure should be taken into account. For the Ewald 3D corrector, we should make the k-space mesh much denser. In conclusion, the molecular dynamic simulation program developed will see a bright future if it is utilized in chemical or bio related fields with better computing support [45].

APPENDIX 1

Initial velocity generator

First we generate 12 uniform random variables, ξ_i, in the range (0,1) and then calculate a random number ξ, to incorporate into velocities

$$\xi = \left(\left(\left(\left(\left(a_9 R^2 + a_7\right)R^2 + a_5\right)R^2 + a_5\right)R^2 + a_3\right)R^2 + a_1\right)R$$

where R is a variable, used to simplify the expression. R is obtained as

$$R = \frac{\left(\sum_{i=1}^{12} \xi_i - 6\right)}{4}$$

Coefficients in (2.29) are given as

$$a_1 = 3.949846138$$

$$a_3 = 0.252408784$$

$$a_5 = 0.076542912$$

$$a_7 = 0.008355968$$

$$a_9 = 0.029899776$$

APPENDIX 2

Fourier Series

Using the method for a generalized Fourier series, the usual Fourier series involving sines and cosines is obtained by taking $f_1(x) = \cos x$ and $f_2(x) = \sin x$. Since these functions form a complete orthogonal system over $[-\pi, \pi]$, the Fourier series of a function $f(x)$ is given by

$$f(x) = \frac{1}{2} a_0 + \sum_{n=1}^{\infty} a_n \cos(n x) + \sum_{n=1}^{\infty} b_n \sin(n x),$$

where the coefficients are

$$\begin{aligned} a_0 &= \frac{1}{\pi} \int_{-\pi}^{\pi} f(x)\, dx \\ a_n &= \frac{1}{\pi} \int_{-\pi}^{\pi} f(x) \cos(n x)\, dx \\ b_n &= \frac{1}{\pi} \int_{-\pi}^{\pi} f(x) \sin(n x)\, dx \end{aligned}$$

And n=1, 2, 3….

Fourier series can also be represented by a complex exponential, using

$e^{i\theta} = \cos\theta + i \sin\theta$, where $i = \sqrt{-1}$. Then $f(x) = \sum_{k=-\infty}^{\infty} \hat{f}_k e^{ikx}$. The coefficients are

$\hat{f}_k = \frac{1}{2}(a_k + ib_k)$, $k \geq 0$ and $\hat{f}_k = \frac{1}{2}(a_{-k} - ib_{-k})$, $k \leq 0$. Or $\hat{f}_k$ can be written as

$$\hat{f}_k = \frac{1}{L} \int_{-L/2}^{+L/2} f(x) e^{-2\pi i k x / L} dx.$$

APPENDIX 3

Reduced units

In molecular dynamics, non-dimensional forms are always used to simplify the calculation procedure. Following is the list of the equations to convert properties to non-dimensional form. Usually, ε, σ, m are used and their values various for different molecules. For the exact values that were used in this work, please find them in table 1

And along with

$$k_b = 1.38 \cdot 10^{-23} \frac{J}{K}$$
$$Na = 6.023 \cdot 10^{23} mole^{-1} \qquad \text{(A.2)}$$
$$\delta t = 2 \cdot 10^{-15} s$$

give conversion to each non-dimensional variable.

Position: $r = \sigma r^*$ (A.3)

Area: $A = (\sigma^2) A^*$ (A.4)

Volume: $V = (\sigma^3) V^*$ (A.5)

Density: $\rho = \rho^* \sigma^{-3}$ (A.6)

Mass: $m_i = (m) m^*$ (A.7)

Number density: $n = \frac{N}{V} = (\sigma^{-3}) \frac{N}{V^*} = (\sigma^{-3}) n^*$ (A.8)

Velocity: $$V = \left(\frac{\varepsilon}{m}\right)^{\frac{1}{2}} V^* \qquad \text{(A.9)}$$

Force: $$f = \left(\frac{\varepsilon}{\sigma}\right) f^* \qquad \text{(A.10)}$$

Energy: $$E = \varepsilon E^* \qquad \text{(A.11)}$$

Electric field: $$E = \varepsilon E^* / \sigma \qquad \text{(A.11)}$$

Pressure: $$P = \left(\varepsilon \sigma^{-3}\right) P^* \qquad \text{(A.12)}$$

Pressure gradient: $$\nabla P = \left(\varepsilon \sigma^{-4}\right) \nabla P^* \qquad \text{(A.13)}$$

Viscosity: $$\mu = \left(\frac{\varepsilon m}{\sigma^4}\right)^{\frac{1}{2}} \mu^* \qquad \text{(A.14)}$$

Strain rate: $$\gamma = \left(\frac{\varepsilon}{\sigma^2 m}\right)^{\frac{1}{2}} \gamma^* \qquad \text{(A.15)}$$

Time: $$t = \left(\frac{\varepsilon}{m\sigma^2}\right)^{-\frac{1}{2}} t^* \qquad \text{(A.16)}$$

Temperature: $$T = \left(\frac{k_b}{\varepsilon}\right)^{-1} T^* \qquad \text{(A.17)}$$

APPENDIX 4

Program flowchart

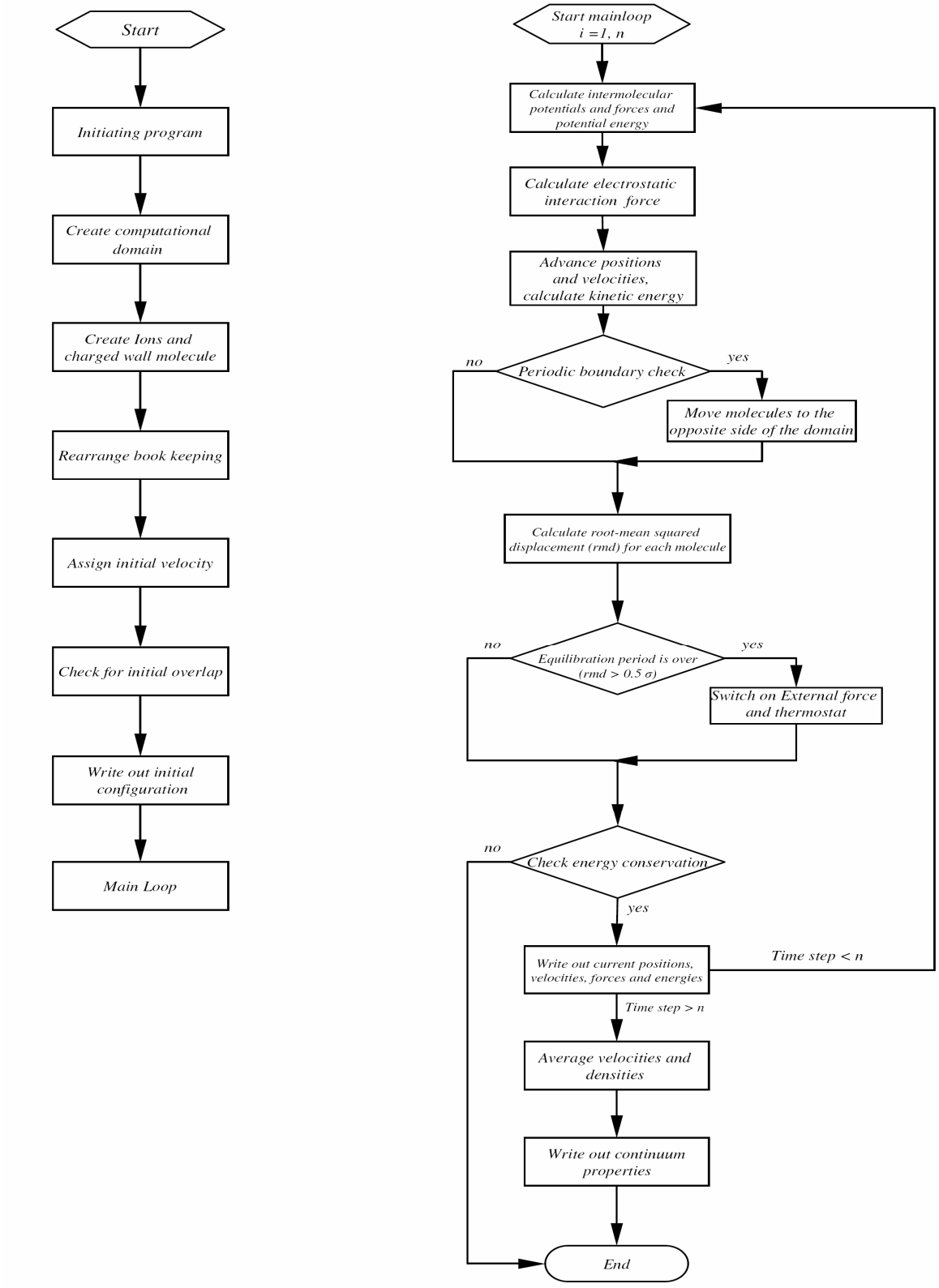

APPENDIX 5

Matlab program used to generate continuum electroosmotic flow velocity

```
clear
clc
i=0
syms t x
for x=0:0.01:1
i=i+1;
a=4;
x1=0.02;
k=1/cosh(a*x1/2);
u=asin( (1/k)/cosh(a/2));
v=asin((1/k)/cosh(a*x/2));
f=double(int(1/sqrt(1-k*sin(t)^2),t,0,pi/2));
f1=double(int(1/sqrt(1-k*sin(t)^2),t,0,u));
f2=double(int(1/sqrt(1-k*sin(t)^2),t,0,v));

Y(i)=1+k*(f1-f2)/4;
Z=k*(f-f1);

X(i)= x;

end
grid
plot(X,Y)
%plot(X1,Y,'-',X2,Y,'o',X3,Y,'.',X5,Y,'ro')
```

BIBLIOGRAPHY

[1] Allen, M.P., Tildesley, D.J., 1987(2002), Computer Simulation of Liquids, Clarendon Press, Oxford.

[2] Fan, X.J., Phan-Thien, N., Yong, N.T., Diao X., 2002, Molecular dynamics simulation of a liquid in a complex nano channel flow, *Physics of Fluids*, vol. **14**, #3, 1146-1153

[3] Haile, J.M., 1993, Molecular Dynamics Simulation: Elementary Methods. New York: Wiley.

[4] Powles, J.G., Murad, S., Ravi, P.V., 1992, A new model for permeable micropores, *Chemical Physics Letters*, vol. **188**, #1,2, 21-23.

[5] Horiuchi, K., Dutta, P., and Hossain, A., 2006, Joule Heating Effects in Mixed Electroosmotic and Pressure Driven Microflows under Constant Wall Heat Flux, *Journal of Engineering Mathematics*, vol. **54**, 159-180.

[6] Lennard-Jones J.E., 1924, The determination of molecular fields, I. From the variation of the viscosity of a gas with temperature, *Proc. Roy. Soc. (London)*, vol. **106A**, 441-462. II. From the equation of state of gas. *Proc. Roy. Soc. (London)*, vol. **106A**, 463-477.

[7] Alder, B. J., Wainwright, T. E., 1957, J. Chem. Phys. vol. **27**, 1208.

[8] Verlet, L. 1967. Computer 'experiments' on classical fluids. I. Thermo dynamical properties of Lennard-Jones molecules. Phys. Rev. 159: 98-103.

[9] Koplik, J., Banavar, J.R., Willemsen, J.F., 1988, Molecular Dynamics of Poiseuille Flow and Moving Contact Lines, *Physical Review Letters*, vol. **60**, #13, 1282-1285.

[10] Koplik, J., Banavar, J.R., 1995, Continuum Deductions from Molecular Hydrodynamics, *Annu. Rev. Fluid Mech*. vol. **27**, 257-292

[11] Todd, B.D., Evans D.J., 1995, The heat flux vector for highly inhomogeneous nonequilibrioum fluids in very narrow pores, *J. Chem. Phys.*, vol. **103** #22, 9804-9809.

[12] Todd, B.D., Evans, D.J., Daivis, P.J., 1995, Pressure tensor for inhomogeneous fluids, *Physical Review E*, vol. **52**, #2, 1627-1638.

[13] Travis, K.P., Gubbins, K.E., 2000, Poiseuille flow of Lennard-Jones fluids in narrow slit pores, *Journal of Chemical Physics*, vol. **112**, #4, 1984-1994

[14] Travis, K.P., Evans, D.J., 1997, Molecular spin in a fluid undergoing Poiseuille flow, *Physical Review E*, vol. **55**, #2, 1566-1572.

[15] Travis, K.P., Todd, B.D., Evans, D.J., 1997, Departure from Navier-Stokes hydrodynamics in confined liquids, *Physical Review E*, vol. **55**, #4, 4288-4294.

[16] Hu, Y., Wang, H., Guo, Y., Zheng, L., 1996, Simulation of lubricant rheology in thin film lubrication. Part I: simulation of Poiseuille flow, Wear, vol. **196**, 243-248, Part II: Simulation of Couette flow, *Wear*, vol. **196**, 249-253.

[17] Berendsen, H.J.C., Grigera, J.R., Straatsma, T.P., 1987, The Missing term in Effective Pair Potentials, *Journal of Physics Chemistry*, vol. **91**, 6269-6271.

[18] Berendsen, H. J. C., 1987, *Comp. Phys. Commun*., vol. **44**, 233.

[19] Nose, S., 1984, A molecular dynamics method for simulations in the canonical ensemble, *Molecular Physics*, 1984, vol. **52**, #2, 255-268

[20] Hoover, W. G., 1985, Canonical dynamics: equilibrium phase-space distributions. *Phys. Review A31*: 1965-97

[21] Ciccotti, G, Hoover, W.G., 1986, Molecular Dynamics Simulation of the Statistical Mechanics Systems. Amsterdam: North Holland.

[22] Ciccotti, G, Frenkel, D and McDonald I., R., 1987, Simulation of liquids and solids*:* A collection of key papers on simulation from the origins to 1986, North-Holland.

[23] Andersen, H., 1980, Molecular Dynamics simulations at constant pressure and/or temperature, *Journal of Chemical Physics*., vol. **72**, # 4, 2384-2393

[24] Burgreen, D., Nakache, F.R., Electrokinetic Flow in Ultrafine Capillary Slits, *J. Phys. Chem.,* vol. **68**, 1084-1091

[25] Freund, J., 2002, Electroosmosis in a nanometer-scale channel studied by atomistic simulation, *Journal of Chemical Physics,* vol. **116**, 2194-2200

[26] Qiao R, Aluru, N.R., 2003, Ion concentrations and velocity profiles in nanochannel electroosmotic flows, *Journal of Chem. Physics*, vol. **118**, #10, 4692-4701

[27] Kim, D., Darve, E., 2006, Molecular dynamics simulation of electro-osmotic flows in rough wall nanochannels, *Physical Review E*, vol. **73,** 051203

[28] Qiao, R., 2006, Effects of molecular level surface roughness on electroosmotic flow, Microfluid Nanofluid, vol. **3**, 33-38

[29] Yeh, I., Berkowitz, M., 1999, Ewald summation for system with slab geometry, *Journal of Chemical Physics*, vol. **111,** 3155-3162.

[30] www.cbe.**buffalo**.edu/courses/ce530/Text/Long_range_**forces**_3.doc

[31] Spohr, E, 1997, Effect of electrostatic boundary conditions and system size on the interfacial properties of water and aqueous solutions, *Journal of Chemical Physics,* vol. **107**, 6342-6348

[32] Scott, W.R.P., Hu¨nenberger, P.H., Tironi, I.G., Mark, Billeter, S.R., Fennen, J., Torda, A.E., Huber, T., Kru¨ger, T., and van Gunsteren, W.F., 1999, The GROMOS biomolecular simulation program package, *Journal of Physics Chemistry* A. vol **103**, 3596–3607

[33] Darden, E., York, E., and Pederson, L., 1993, Particle mesh Ewald: An $N\cdot\log(N)$ method for Ewald sums in large systems, *Journal of Chemical Physics,* vol. **98**, 10089-10092.

[34] Essmann, U., Perera, L., Berkowitz, M. L., Darden, T., Lee, H., and Pedersen, L. G., 1995, A smooth particle mesh Ewald method, *Journal of Chemical Physics*, vol. **103**, 8577.

[35] Smith, E.R., 1981, Electrostatic Energy in Ionic crystal, *Proc. Roy. Soc. London, Ser. A* vol. **375**, 475

[36] Spohr, E., 1999, Molecular Simulation of the electrochemical double layer, *Electrochimica Acta*, vol. **44**, 1697-1705.

[37] Markus D., Christain., 1998, How to mesh up Ewald sums. I.A theotetical and numerical comparison of various particles mesh routines, *Journal of Chemical Physics*, vol. **109**, 7678-7693

[38] Deserno, M., Holm, C., 1998, How to mesh up Ewald sums. I.A theotetical and numerical comparison of various particles mesh routines, *Journal of Chemical Physics*, vol. **109**, 7678-7693.

[39] Crozier, P.S., Rowley, R.L., Holladay, N.B., Henderson, D., Busath D.D., 2001, Molecular Dynamics Simulation of Continuous Current Flow through a Model Biological Membrane Channel, *Physical Review Letters*, vol. **86**, #11, 2467-2470

[40] Crozier, P.S., Rowley, R.L., Henderson, D., 2001, Molecular-dynamics simulations of ion size effects on the fluid structure of aqueous electrolyte systems between charged model electrodes, *Journal of Chemical Physics*, vol. **114**, # 17, 7513-7517.

[41] Cui, S.T., and Cochran, H.D., 2003, Electroosmotic flow in nanoscale parallel plate channels: Molecular Simulation study and comparison with classical Poisson-Boltzmann Theory, *Molecular Simulation*, vol. **30** (5), 259-266.

[42] Zhu,W., Singer, S., 2005, Electroosmotic flow of a model electrolyte, *Phycisal Review E*, vol. **71**, 04501-1-12

[43] Foiles, S. M., Baskes M. I., Daw M. S., 1986, Embedded atom method functions for the fcc metals and their alloys. *Phys. Review B,* vol. **33**: 7983-7991

[44] Rappaport, D. C., 1988, Large-scale molecular dynamics simulation using vector and parallel computers. *Comput. Physics Rep*., vol. **9**:1-53

[45] Lyklema, J., Rovillard, S., De Coninck, J., 1998, Electrokinetics: The Properties of the Stagnant Layer Unraveled, *The ACS Journal of Surfaces and Colloids*, vol. **14**, #20, 5659-5663.